Journal of

Mechanics of

Materials and Structures

INTERACTION OF A DISLOCATION WITH COLLINEAR RIGID
LINES AT THE INTERFACE OF PIEZOELECTRIC MEDIA

ZhongMin Xiao, Hongxia Zhang and Bingjin Chen

INTERACTION OF A DISLOCATION WITH COLLINEAR RIGID LINES AT THE INTERFACE OF PIEZOELECTRIC MEDIA

ZHONGMIN XIAO, HONGXIA ZHANG AND BINGJIN CHEN

This paper investigates the electroelastic interaction between a dislocation and collinear interfacial rigid lines in two dissimilar piezoelectric materials subjected to remote loadings. Both conducting and dielectric rigid lines are considered. The general solutions for the field variables are obtained based on the Stroh formalism and analytical function theory. The stress and electric displacement fields at the tips of rigid conducting lines are present as either a square root singularity or a combination of any two of the three kinds of singularities: square root singularity, nonsquare root singularity and oscillatory singularity. The stress and electric displacement fields at the tips of rigid dielectric lines exhibit either a square root singularity or a combination of square root and oscillatory singularities. Singularities depend on the electroelastic properties of the two piezoelectric materials. The rigid line extension force is expressed in terms of the strain and electric field intensity factors which are analogous to the stress and electric displacement intensity factors defined for interfacial cracks. The exact field solutions for the case of a single interfacial rigid line are presented. The tangential and radial components of the image force on the dislocation are calculated. Numerical examples are presented to demonstrate the effects of some important parameters on the image force.

1. Introduction

Piezoelectric materials are widely used as sensors, actuators, and electromechanical devices due to their inherent electromechanical coupling behavior. However, defects such as dislocations, cracks, cavities, and inclusions can adversely influence the performance of such piezoelectric devices. Therefore it is of great importance to investigate the behaviors of various defects in electroelastic fields in order to understand the fracture behaviors of these materials and predict the integrity of theses devices.

Many efforts have been devoted to the crack models in piezoelectric materials [Pak 1990a; Sosa and Pak 1990; Suo et al. 1992]. Suo et al. [1992] analyzed the generalized two dimensional problem of an interfacial impermeable crack in piezoelectric bimaterials. They discovered that the crack tip fields show the type of singularities of order $r^{-1/2\pm i\varepsilon}$ and $r^{-1/2\mp\kappa}$. Ou and Wu [2003] further proved that either ε or κ is equal to zero for the problem of an interfacial impermeable crack in a transversely isotropic piezoelectric bimaterial system. Beom [2003] and Hausler et al. [2004] examined a permeable crack at the interface of two piezoelectric media and identified an oscillatory singularity for the fields. Beom and Atluri [2002] derived two pairs of oscillatory singularities for the fields around an interfacial conducting crack tip in piezoelectric bimaterials. Ru [2000] studied a conducting crack between electrode layers and piezoelectric ceramics. He identified a square root singularity for the tip tensile stress and a nonsquare root singularity for the shear stress. Wang and Shen [2002] gave a general treatment on various interfacial

defects in piezoelectric media. Xiao and Zhao [2004] analyzed a Zener–Stroh crack at the interface of metal/piezoelectric bimaterials by means of Green's function. Contributions have also been made to study the dislocation-inclusion/interface/crack interaction in piezoelectric materials, for example [Meguid and Deng 1998; Xiao et al. 2004; Fang et al. 2005; Chen et al. 2005a; Chen et al. 2005b] and [Gao et al. 2005].

Rigid line problems also attract researchers' attention. Some solutions for the problems of rigid lines in purely elastic materials under mechanical loading were obtained by Li and Ting [1989], Jiang [1991], Ballarini [1990], Wu [1990], Jiang and Liu [1992], and Asundi and Deng [1995]. The stresses possess a pronounced oscillatory character at the tip of interfacial rigid lines. Deng and Meguid [1998] analyzed all the possible singularities of the field variables at an interfacial rigid conducting line tip in piezoelectric materials loaded at infinity. Recently, the interactions of a screw dislocation with interfacial rigid lines in piezoelectric solids have been studied by Liu et al. [2004] and Xiao et al. [2007]. Chen et al. [2007] examined the interaction of a dislocation with collinear rigid lines in a piezoelectric solid. To our knowledge, however, no attempt has been made to investigate the generalized two-dimensional interaction between a dislocation and interfacial rigid lines in piezoelectric media.

The current work presents the interactive solution for a dislocation and collinear rigid lines at the interface of two piezoelectric materials. Rigid conducting and dielectric lines are modeled. The field solutions and the near-tip singularities are discussed in detail in Section 4 and Section 5. The generalized strain intensity factors are introduced to characterize the near-tip fields and rigid line extension forces are obtained. In Section 6, the exact solutions for a special case of a single interfacial rigid line are given. The image force on the dislocation is calculated in Section 7. In Section 8, the influences of some important parameters, such as the Burgers vector and dislocation position, on the image force are analyzed. A conclusion is given in Section 9.

2. Stroh formalism

Consider a linear piezoelectric solid in a Cartesian coordinate system (x_1, x_2, x_3). For a two-dimensional problem where all the field variables depend on x_1 and x_2 only, a general solution can be expressed as

$$\boldsymbol{u} = \boldsymbol{A}\boldsymbol{f}(z) + \bar{\boldsymbol{A}}\overline{\boldsymbol{f}(z)}, \qquad \boldsymbol{\Phi} = \boldsymbol{B}\boldsymbol{f}(z) + \bar{\boldsymbol{B}}\overline{\boldsymbol{f}(z)},$$

with

$$\boldsymbol{u} = [u_1, u_2, u_3, u_4]^T, \quad \boldsymbol{\Phi} = [\phi_1, \phi_2, \phi_3, \phi_4]^T,$$

$$\boldsymbol{f}(z) = [f_1(z), f_2(z), f_3(z), f_4(z)]^T.$$

In the above equations, $\boldsymbol{u}$ and $\boldsymbol{\Phi}$ denote the generalized displacement and stress function vectors, respectively, $\boldsymbol{A}$ and $\boldsymbol{B}$ are the 4×4 matrices determined from material constants, and $\boldsymbol{f}(z)$ is a function vector to be found. For simplicity, each component of $\boldsymbol{f}(z)$ is considered to be a function of one complex variable z instead of $z_\alpha = x_1 + p_\alpha x_2$ ($\alpha = 1, 2, 3, 4$) [Suo et al. 1992], where p_α is a complex eigenvalue with positive imaginary part. Thus, the generalized strains (strain and electric field) and the generalized

stresses (stress and electric displacement) are given by

$$\boldsymbol{u}_{,1} = \left[u_{j,1}, -E_1\right]^T = \boldsymbol{A}\boldsymbol{f}(z) + \bar{\boldsymbol{A}}\overline{\boldsymbol{F}(z)}, \tag{1}$$

$$\boldsymbol{\Phi}_{,1} = \left[\sigma_{2j}, D_2\right]^T = \boldsymbol{B}\boldsymbol{F}(z) + \bar{\boldsymbol{B}}\overline{\boldsymbol{F}(z)}, \tag{2}$$

$$\boldsymbol{\Phi}_{,2} = \left[\sigma_{1j}, D_1\right]^T = \boldsymbol{B}\langle p_\alpha\rangle\boldsymbol{F}(z) + \overline{\boldsymbol{B}\langle p_\alpha\rangle\boldsymbol{F}(z)}, \tag{3}$$

respectively, where a comma denotes partial differentiation and $\boldsymbol{F}(z) = d\boldsymbol{f}(z)/dz$. when calculating the field variables, z should be replaced by z_α for the αth component function.

The matrices $\boldsymbol{A}$ and $\boldsymbol{B}$, when properly normalized, satisfy the orthogonality relation:

$$\begin{bmatrix} \boldsymbol{B}^T & \boldsymbol{A}^T \\ \bar{\boldsymbol{B}}^T & \bar{\boldsymbol{A}}^T \end{bmatrix} \begin{bmatrix} \boldsymbol{A} & \bar{\boldsymbol{A}} \\ \boldsymbol{B} & \bar{\boldsymbol{B}} \end{bmatrix} = \begin{bmatrix} \boldsymbol{I} & \boldsymbol{0} \\ \boldsymbol{0} & \boldsymbol{I} \end{bmatrix}, \tag{4}$$

where $\boldsymbol{I}$ is a 4×4 identity matrix. The three matrices $\boldsymbol{S}$, $\boldsymbol{H}$, and $\boldsymbol{L}$ are defined by

$$\boldsymbol{H} = i2\boldsymbol{A}\boldsymbol{A}^T, \qquad \boldsymbol{L} = i2\boldsymbol{B}\boldsymbol{B}^T, \qquad \boldsymbol{S} = i(\boldsymbol{A}\boldsymbol{B}^T - \boldsymbol{I}),$$

respectively. In addition, Hermitian matrix $\boldsymbol{M}$, which appears in the analysis, is defined by

$$\boldsymbol{M} = -i\boldsymbol{B}\boldsymbol{A}^{-1} = \boldsymbol{H}^{-1} + i\boldsymbol{H}^{-1}\boldsymbol{S}.$$

For convenience, a Hermitian matrix $\boldsymbol{Y}$ involving bimaterial properties is defined as

$$\boldsymbol{Y} = \boldsymbol{M}_1 + \bar{\boldsymbol{M}}_2,$$

where the subscripts 1 and 2 attached to matrices and vectors distinguish the two materials. The elements of $\boldsymbol{Y}$ are represented by Y_{ij}. We introduce a 3×3 bimaterial matrix $\hat{\boldsymbol{Y}}$ with the elements $\hat{Y}_{ij}$ given by

$$\hat{Y}_{ij} = Y_{ij} - \frac{1}{Y_{44}}Y_{i4}Y_{4j}. \tag{5}$$

It is easily shown from Equation (5) that

$$\hat{Y}_{ij}^{-1} = Y_{ij}^{-1}, \qquad i, j = 1, 2, 3, \tag{6}$$

where $\hat{Y}_{ij}^{-1}$ and Y_{ij}^{-1} denotes the elements of matrices $\hat{\boldsymbol{Y}}^{-1}$ and $\boldsymbol{Y}^{-1}$, respectively. It can be shown that $\hat{\boldsymbol{Y}}$ is a positive definite Hermitian matrix by using the properties of $\boldsymbol{Y}$.

3. Statement of the problem

Consider a piezoelectric dislocation with Burgers vector $\boldsymbol{b} = \left[b_1, b_2, b_3, b_\varphi\right]^T$ located at $z_d = x_{1d} + ix_{2d}$ in the upper half-infinite plane s_1, as shown in Figure 1. The dislocation core is subjected to a line load $\boldsymbol{f} = \left[-p_1, -p_2, -p_3, q\right]^T$. Suppose there are collinear rigid lines l_k ($k = 1, 2, \ldots, n$) with end points a_k and b_k at the interface of s_1 and the lower half-infinite plane s_2, with the plane subjected to the uniform loading at infinity. Let L_l and L_b denote the unions of rigid lines and perfectly bonded parts along the x_1 axis, respectively.
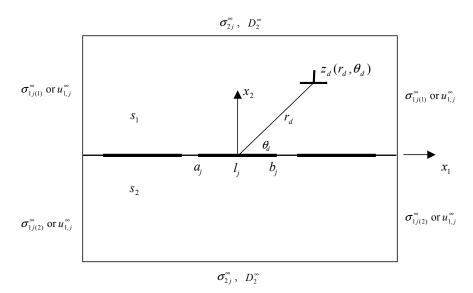
Figure 1. A piezoelectric dislocation near collinear rigid line inclusions at the interface of two dissimilar piezoelectric media.

The mechanical boundary and equilibrium conditions of interfacial rigid lines are

$$u_{j,1}^+(x_1) = u_{j,1}^-(x_1) = \delta_{j2}\omega_k, \qquad j = 1, 2, 3, \quad k = 1, 2, \ldots, n, \qquad \text{on } L_l, \tag{7}$$

$$\int_{L_l} (\sigma_{2j}^+(x_1) - \sigma_{2j}^-(x_1))dx_1 = 0, \qquad j = 1, 2, 3, \qquad \text{on } L_l, \tag{8}$$

$$\int_{L_l} (\sigma_{22}^+(x_1) - \sigma_{22}^-(x_1))x_1 dx_1 = 0, \qquad \text{on } L_l, \tag{9}$$

where ω_k are unknown constants which represent the rotation of the kth rigid line, and the superscripts + and − refer to the boundary values from s_1 and s_2, respectively.

Assuming zero thickness of rigid lines, the electric boundary conditions are described as

$$E_1^+(x_1) = E_1^-(x_1) = 0, \qquad \text{on } L_l, \tag{10}$$

$$\int_{L_l} (D_2^+(x_1) - D_2^-(x_1))dx_1 = 0, \qquad \text{on } L_l, \tag{11}$$

for the conducting case, and

$$E_1^+(x_1) = E_1^-(x_1), \qquad \text{on } L_l, \tag{12}$$

$$D_2^+(x_1) = D_2^-(x_1), \qquad \text{on } L_l \tag{13}$$

for the dielectric case.

The boundary conditions along perfectly bonded parts are

$$u_j^+(x_1) = u_j^-(x_1), \qquad j = 1, 2, 3, 4, \qquad \text{on } L_b, \tag{14}$$

$$\sigma_{2j}^+(x_1) = \sigma_{2j}^-(x_1), \qquad D_2^+(x_1) = D_2^-(x_1), \qquad j = 1, 2, 3, \qquad \text{on } L_b. \tag{15}$$

4. Formulation and solution

Let $\boldsymbol{F}_1(z)$ and $\boldsymbol{F}_2(z)$ be the complex potentials in s_1 and s_2, respectively. Based on the superposition principle, we can express

$$\boldsymbol{F}_k(z) = \boldsymbol{F}_k^\infty + \boldsymbol{F}_{ka}(z) + \boldsymbol{F}_{kb}(z), \qquad k = 1, 2, \tag{16}$$

where constant vectors $\boldsymbol{F}_k^\infty$ are determined by the uniform loading at infinity in the absence of rigid lines, $\boldsymbol{F}_{ka}(z)$ are the complex potentials due to the interaction of a dislocation with a perfectly bonded interface. The complex potentials $\boldsymbol{F}_{kb}(z)$ correspond to the perturbed field due to collinear interfacial rigid lines. $\boldsymbol{F}_{ka}(z)$ and $\boldsymbol{F}_{kb}(z)$ vanish at infinity.

We begin with the perfectly bonded interface problem in the absence of rigid lines. Such loadings $\boldsymbol{\Phi}_{,1}^\infty = \left[\sigma_{21}^\infty, \sigma_{22}^\infty, \sigma_{23}^\infty, D_2^\infty\right]^T$ and $\boldsymbol{u}_{,1}^\infty = \left[\varepsilon_{11}^\infty, \varepsilon_{12}^\infty + \omega^\infty, 2\varepsilon_{13}^\infty, -E_1^\infty\right]^T$ are applied that the continuous conditions on tractions and displacements at the interface are satisfied. Thus, from Equation (1) and (2), we have

$$\boldsymbol{A}_k \boldsymbol{F}_k^\infty + \bar{\boldsymbol{A}}_k \bar{\boldsymbol{F}}_k^\infty = \boldsymbol{u}_{,1}^\infty, \qquad \boldsymbol{B}_k \boldsymbol{F}_k^\infty + \bar{\boldsymbol{B}}_k \bar{\boldsymbol{F}}_k^\infty = \boldsymbol{\Phi}_{,1}^\infty, \qquad k = 1, 2, \ -\infty < x_1 < \infty. \tag{17}$$

In view of Equation (4) and (17), one has

$$\boldsymbol{F}_k^\infty = \boldsymbol{A}_k^T \boldsymbol{\Phi}_{,1}^\infty + \boldsymbol{B}_k^T \boldsymbol{u}_{,1}^\infty, \qquad k = 1, 2.$$

Tractions and displacements are continuous along the entire x_1 axis, so that

$$\boldsymbol{u}_{a,1}^+(x_1) = \boldsymbol{u}_{a,1}^-(x_1), \qquad \boldsymbol{\Phi}_{a,1}^+(x_1) = \boldsymbol{\Phi}_{a,1}^-(x_1), \qquad -\infty < x_1 < \infty, \tag{18}$$

where $\boldsymbol{u}_{a,1}$ and $\boldsymbol{\Phi}_{a,1}$ denote the generalized strains and stresses due to the dislocation at z_d, respectively. For this subproblem, the solution can be given by

$$\boldsymbol{F}_a(z) = \begin{cases} \boldsymbol{F}_{1d}(z) + \boldsymbol{F}_{10}(z), & z \in s_1, \\ \boldsymbol{F}_{20}(z), & z \in s_2, \end{cases} \tag{19}$$

where $\boldsymbol{F}_{1d}(z)$ is the solution for a dislocation at z_d in an infinite plane given by

$$\boldsymbol{F}_{1d}(z) = \frac{1}{2\pi i} \left\langle \frac{1}{z - z_{d\alpha}} \right\rangle (\boldsymbol{B}_1^T \boldsymbol{b} + \boldsymbol{A}_1^T \boldsymbol{f}). \tag{20}$$

The above bracket $\langle \ \rangle$ denotes a diagonal matrix. With the arguments of [Suo et al. 1992], one finds

$$\boldsymbol{F}_{10}(z) = \boldsymbol{A}_1^{-1} \boldsymbol{Y}^{-1} (\bar{\boldsymbol{M}}_1 - \bar{\boldsymbol{M}}_2) \bar{\boldsymbol{A}}_1 \bar{\boldsymbol{F}}_{1d}(z), \tag{21}$$

$$\boldsymbol{F}_{20}(z) = 2\boldsymbol{A}_2^{-1} \bar{\boldsymbol{Y}}^{-1} \boldsymbol{H}_1^{-1} \boldsymbol{A}_1 \boldsymbol{F}_{1d}(z). \tag{22}$$

The substitution of the above equations into Equation (19) gives the complete solution.

Consider the rigid lines disturbed subproblem. From Equations (7), (10) or (12), and (14), the displacement continuities along the x_1 axis, along with Equations (1), (16), (17) and (18), give

$$A_1 F_{1b}^+(x_1) + \bar{A}_1 \bar{F}_{1b}^-(x_1) = A_2 F_{2b}^-(x_1) + \bar{A}_2 \bar{F}_{2b}^+(x_1), \qquad -\infty < x_1 < \infty. \tag{23}$$

By the analytic continuity argument, it follows that

$$\begin{cases} A_1 F_{1b}(z) = \bar{A}_2 \bar{F}_{2b}(z), & z \in s_1, \\ A_2 F_{2b}(z) = \bar{A}_1 \bar{F}_{1b}(z), & z \in s_2. \end{cases} \tag{24}$$

With such representations, the generalized stress jumps across rigid lines are obtained as

$$\Delta \boldsymbol{\Phi}_{,1}(x_1) = i Y \left[\boldsymbol{I}^+(x_1) - \boldsymbol{I}^-(x_1) \right], \tag{25}$$

where

$$\boldsymbol{I}(z) = \begin{cases} A_1 F_{1b}(z), & z \in s_1, \\ Y^{-1} \bar{Y} A_2 F_{2b}(z), & z \in s_2. \end{cases} \tag{26}$$

Since $\Delta \boldsymbol{\Phi}_{,1}(x_1) = 0$ on L_b from Equation (15), (25) shows that

$$\boldsymbol{I}(z) = \left[I_1(z), I_2(z), I_3(z), I_4(z) \right]^T$$

is analytic in the entire plane except at the rigid lines.

Substituting Equation (16) into (1) with (17) gives

$$\boldsymbol{u}_{,1}(x_1) = \boldsymbol{u}_{,1}^\infty + \boldsymbol{u}_{a,1}(x_1) + \boldsymbol{I}^+(x_1) + \bar{Y}^{-1} Y \boldsymbol{I}^-(x_1), \tag{27}$$

where

$$\boldsymbol{u}_{a,1}(x_1) = \frac{2}{\pi} \operatorname{Im} \left[N \left\langle \frac{1}{x - z_{d\alpha}} \right\rangle \boldsymbol{d} \right]. \tag{28}$$

In the above equation, $N = \bar{Y}^{-1} H_1^{-1} A_1$ and $\boldsymbol{d} = B_1^T \boldsymbol{b} + A_1^T \boldsymbol{f}$, which are defined for simplicity. The elements of matrix N and vector $\boldsymbol{d}$ are represented by N_{ij} ($i, j = 1, 2, 3, 4$) and d_i ($i = 1, 2, 3, 4$), respectively. Once $\boldsymbol{I}(z)$ is found, so is the full field.

The solution is simple if Y is real. When the collinear rigid lines are in a homogeneous material, Y is indeed real. Y can be real for bimaterials having sufficient symmetry. In the following, real Y is assumed in Sections 4.1 and 4.2, and the case that Y is complex is examined in Sections 4.3 and 4.4.

4.1. *Rigid conducting lines: the fields of a square root singularity.* With real Y, from Equations (7), (10) and (27), one has

$$\boldsymbol{I}^+(x_1) + \boldsymbol{I}^-(x_1) = \boldsymbol{\Omega} - \boldsymbol{u}_{,1}^\infty - \boldsymbol{u}_{a,1}(x_1), \qquad \text{on } L_l, \tag{29}$$

where

$$\boldsymbol{\Omega} = \begin{cases} [0, \omega_1, 0, 0]^T, & \text{on } l_1, \\ \cdots\cdots \\ [0, \omega_n, 0, 0]^T, & \text{on } l_n. \end{cases} \tag{30}$$

The general solution can be obtained from the method of [Muskhelishvili 1975] as

$$
\boldsymbol{I}(z) = \frac{1}{2}X(z)\left\{ \oint_{\eta} \frac{\boldsymbol{\Omega}}{X(\xi)(\xi - z)} d\xi - \boldsymbol{u}_{,1}^{\infty}\left[\frac{1}{X(z)} - x(\infty) \right] \right.
$$

$$
- \frac{1}{\pi i}\boldsymbol{N}\left\langle \frac{1}{(z_{\alpha} - z_{d\alpha})X(z_{\alpha})} - 1 - \frac{1}{(z_{\alpha} - z_{d\alpha})X(z_{d\alpha})} \right\rangle \boldsymbol{d}
$$

$$
\left. + \frac{1}{\pi i}\bar{\boldsymbol{N}}\left\langle \frac{1}{(z_{\alpha} - \bar{z}_{d\alpha})X(z_{\alpha})} - \frac{1}{(z_{\alpha} - \bar{z}_{d\alpha})X(\bar{z}_{d\alpha})} - 1 \right\rangle \bar{\boldsymbol{d}} + \boldsymbol{P}^{a}(z) \right\}, \quad (31)
$$

where

$$
\boldsymbol{P}^{a}(z) = \boldsymbol{c}_{n-1}^{a} z^{n-1} + \cdots + \boldsymbol{c}_{0}^{a}, \tag{32}
$$

$$
X(z) = \prod_{j=1}^{n} (z - a_j)^{-1/2}(z - b_j)^{-1/2}, \tag{33}
$$

$$
x(\infty) = \prod_{j=1}^{n} \left[z - (a_j + b_j)/2 \right], \tag{34}
$$

in which η is the union of the n contours $\eta_1, \ldots, \eta_n$, surrounding the rigid lines $L_1, \ldots, L_n$ in clockwise direction.

From Equations (8), (11) and (25), we can obtain the closed path integral

$$
\oint_{\eta_j} \boldsymbol{I}(z)dz = \boldsymbol{0}, \qquad j = 1, 2, \ldots, n. \tag{35}
$$

One has from Equations (9) and (25) the closed path integral

$$
\boldsymbol{Y}^{(2)} \oint_{\eta_j} \boldsymbol{I}(z)dz = 0, \qquad j = 1, 2, \ldots, n. \tag{36}
$$

The n vectors $\boldsymbol{c}_{j-1}^{a}$ and n constants ω_j ($j = 1, 2, \ldots, n$) can be obtained by substituting Equation (31) into Equations (35) and (36) with Equations (32)–(34). $\boldsymbol{F}_{kb}(z)$ can be found by using Equation (26).

4.2. *Rigid dielectric lines: the fields of a square root singularity.* The condition, Equation (13), along the rigid dielectric lines leads to

$$
\boldsymbol{Y}^{(4)}\boldsymbol{I}(z) = 0. \tag{37}
$$

One has from Equation (37) that

$$
I_4(z) = -\frac{Y_{4j}}{Y_{44}} I_j(z), \qquad j = 1, 2, 3. \tag{38}
$$

Thus we have

$$
\boldsymbol{I}(z) = (\hat{\boldsymbol{I}} - \boldsymbol{E})\hat{\boldsymbol{I}}(z), \tag{39}
$$

where $\hat{\boldsymbol{I}}(z) = \left[I_1(z), I_2(z), I_3(z)\right]^T$, $\hat{\boldsymbol{I}}$ is obtained by deleting the fourth column from a 4×4 identity matrix, and $\boldsymbol{E} = \left[\boldsymbol{E}_1, \boldsymbol{E}_2, \boldsymbol{E}_3\right]$ with $\boldsymbol{E}_i = \left[0, 0, 0, Y_{4i}/Y_{44}\right]^T$. The relations in Equations (37)–(39) are valid for real and complex $\boldsymbol{Y}$.

With real $\boldsymbol{Y}$, Equations (5), (6), (7), (27) and (39) lead to

$$\hat{\boldsymbol{I}}^+(x_1) + \hat{\boldsymbol{I}}^-(x_1) = \hat{\boldsymbol{\Omega}} - \hat{\boldsymbol{u}}_{,1}^\infty - \hat{\boldsymbol{u}}_{a,1}(x_1), \tag{40}$$

where

$$\hat{\boldsymbol{\Omega}} = \begin{cases} \left[0, \omega_1, 0\right]^T, & \text{on } l_1, \\ \cdots \cdots \\ \left[0, \omega_n, 0\right]^T, & \text{on } l_n, \end{cases} \tag{41}$$

$$\hat{\boldsymbol{u}}_{,1}^\infty = \left[u_{1,1}^\infty, u_{2,1}^\infty, u_{3,1}^\infty\right]^T, \qquad \hat{\boldsymbol{u}}_{a,1} = \left[u_{1,1}^a, u_{2,1}^a, u_{3,1}^a\right]^T.$$

The general solution to Equation (40) is given by

$$\begin{aligned}
\hat{\boldsymbol{I}}(z) = \frac{1}{2}X(z)\Bigg\{ & \oint_\eta \frac{\hat{\boldsymbol{\Omega}}}{X(\xi)(\xi - z)}d\xi - \hat{\boldsymbol{u}}_{,1}^\infty\left[\frac{1}{X(z)} - x(\infty)\right] \\
& - \frac{1}{\pi i}\hat{\boldsymbol{N}}\left\langle \frac{1}{(z_\alpha - z_{d\alpha})X(z_\alpha)} - 1 - \frac{1}{(z_\alpha - z_{d\alpha})X(z_{d\alpha})} \right\rangle \boldsymbol{d} \\
& + \frac{1}{\pi i}\bar{\hat{\boldsymbol{N}}}\left\langle \frac{1}{(z_\alpha - \bar{z}_{d\alpha})X(z_\alpha)} - \frac{1}{(z_\alpha - \bar{z}_{d\alpha})X(\bar{z}_{d\alpha})} - 1 \right\rangle \bar{\boldsymbol{d}} + \boldsymbol{P}^b(z) \Bigg\}, \tag{42}
\end{aligned}$$

where $\hat{\boldsymbol{N}}$ is a 3×4 matrix obtained by deleting the fourth row of matrix $\boldsymbol{N}$ and

$$\boldsymbol{P}^b(z) = \boldsymbol{c}_{n-1}^b z^{n-1} + \cdots + \boldsymbol{c}_0^b. \tag{43}$$

Using Equations (8), (25) and (39), we can obtain the closed path integral

$$\oint_{\eta_j} \hat{\boldsymbol{I}}(z)dz = \boldsymbol{0}, \qquad j = 1, 2, \ldots, n. \tag{44}$$

From Equations (5), (9), (25), and (39), one has the closed path integral

$$\hat{\boldsymbol{Y}}^{(2)} \oint_{\eta_j} \hat{\boldsymbol{I}}(z)z\,dz = 0, \qquad j = 1, 2, \ldots, n, \tag{45}$$

where $\hat{\boldsymbol{Y}}^{(2)} = \left[\hat{Y}_{21}, \hat{Y}_{22}, \hat{Y}_{23}\right]$. Substituting Equation (42) into Equations (44) and (45), with Equations (33), (34), and (43), we have the n vectors $\boldsymbol{c}_{j-1}^b$ and the n constants ω_j ($j = 1, 2, \ldots, n$). Then, we can find $\boldsymbol{F}_{kb}(z)$ by using Equation (26).

For both conducting and dielectric cases, we can evaluate the generalized strain and stress intensity factors at the right tip of the jth rigid line as

$$k = [k_1, k_2, k_3, k_4]^T = \lim_{x \to b_j} \sqrt{2\pi(x - b_j)}(I(x) + \bar{I}(x)), \tag{46}$$

$$K = [K_{II}, K_I, K_{III}, K_D]^T = \lim_{x \to b_j} \sqrt{2\pi(x - b_j)}[iM_1I(x) - i\bar{M}_1\bar{I}(x)], \tag{47}$$

respectively. For the dielectric case, Equation (46), in view of (39), can be rewritten as

$$k = (\hat{I} - E)\hat{k}, \tag{48}$$

where

$$\hat{k} = [k_1, k_2, k_3]^T = \lim_{x \to b_j} \sqrt{2\pi(x - b_j)}[\hat{I}(x) + \bar{\hat{I}}(x)]. \tag{49}$$

Thus, the generalized strains at the interface a distance r ahead of the tip, and the generalized stress jumps a distance r behind the tip, of the jth rigid line, are given by

$$u(r) = (2r/\pi)^{1/2}k, \tag{50}$$

$$\Delta\Phi_{,1}(r) = (1/2\pi r)^{1/2}Yk, \tag{51}$$

respectively. For the dielectric case, Equation (51) can be further rewritten as

$$[\Delta\sigma_{21}(r), \Delta\sigma_{22}(r), \Delta\sigma_{23}(r)]^T = (1/2\pi r)^{1/2}\hat{Y}\hat{k}, \qquad \Delta D_2(r) = 0. \tag{52}$$

In view of Equation (47), the generalized stresses at the interface a distance r ahead of the jth rigid line tip are given by

$$[\sigma_{2j}(r), D_2(r)]^T = (2\pi r)^{-1/2}K. \tag{53}$$

It is interesting to note that Equation (50) has the same structure as the expression of the generalized stresses ahead of an impermeable crack tip and (51) has the same structure as that of the generalized displacement jumps behind the crack tip [Suo et al. 1992].

Furthermore, the rigid line extension force can be calculated by the closure integral

$$G = \lim_{\delta \to 0} -\frac{1}{2\delta} \int_0^\delta \Delta\Phi_{,1}^T(r)u(\delta - r)dr. \tag{54}$$

Substituting Equations (50) and (51) into (54) leads to

$$G = -\frac{1}{4}k^T Yk. \tag{55}$$

For the dielectric case, Equation (55) can be further rewritten as

$$G = -\frac{1}{4}\hat{k}^T \hat{Y}\hat{k}. \tag{56}$$

It should be pointed out that all the results in Section 4.1 and Section 4.2 are applied to the corresponding problems of collinear rigid conducting and dielectric lines in a homogeneous piezoelectric material, where $M_1 = M_2$ and $Y = 2H_1^{-1}$.

4.3. *Rigid conducting lines: the fields of square root, nonsquare root and oscillatory singularities.*
For complex Y, Equations (7), (10), and (27) lead to

$$I^+(x_1) + \bar{Y}^{-1}YI^-(x_1) = \Omega - u^\infty_{,1} - u_{a,1}(x_1), \qquad \text{on } L_l. \tag{57}$$

Assuming that the eigenvalues of $\bar{Y}^{-1}Y$ take the form $-e^{2\pi i\delta_\alpha}$ with $\delta_\alpha = -1/2 + i\varepsilon_\alpha$, we have

$$\varepsilon_{1,2} = \pm\varepsilon, \qquad \varepsilon_{3,4} = \mp i\kappa, \tag{58}$$

where

$$\varepsilon = \tanh^{-1}(\beta_1)/\pi, \qquad \kappa = \tan^{-1}(-i\beta_2)/\pi,$$

$$\beta_1 = \left[(b^2 - c)^{1/2} - b\right]^{1/2}, \qquad \beta_2 = i[(b^2 - c)^{1/2} + b]^{1/2},$$

$$b = \text{tr}\,[(D^{-1}U)^2]/4, \qquad c = ||D^{-1}U||,$$

$$D = \text{Re}\,[Y], \qquad U = \text{Im}\,[Y].$$

Let Λ_α be the eigenvector of $\bar{Y}^{-1}Y$ corresponding to the eigenvalue $-e^{2\pi i\delta_\alpha}$. Suo et al. [1992] assumed that both values of ε and κ are nonzero and four linearly independent eigenvectors would be obtained for impermeable cracks in a piezoelectric bimaterial system. Here, three combinations of ε and κ are considered:

$$\textbf{case 1}: \quad \varepsilon \neq 0 \ (b \neq 0), \kappa \neq 0 \ (c \neq 0),$$
$$\textbf{case 2}: \quad \varepsilon \neq 0 \ (b < 0), \kappa = 0 \ (c = 0),$$
$$\textbf{case 3}: \quad \varepsilon = 0 \ (b > 0), \kappa \neq 0 \ (c = 0).$$

It can be identified that the eigenvectors Λ_1 and Λ_2 are complex conjugates, that is, $\Lambda_2 = \bar{\Lambda}_1$, and Λ_3 and Λ_4 are real for cases 1 and 2, and all of them are real for case 3 [Deng and Meguid 1998]. Ou and Wu [2003] confirmed that cases 2 and 3 apply to the problem of an impermeable interfacial crack in a transversely isotropic piezoelectric bimaterial system. Four linearly independent eigenvectors can be obtained for the three cases. For simplicity, we define

$$\Lambda_A = \left[\Lambda_1, \Lambda_2, \Lambda_3, \Lambda_4\right], \qquad \Lambda_B = \begin{cases} [\bar{\Lambda}_1, \Lambda_1, \Lambda_4, \Lambda_3], & \text{for case 1,} \\ [\bar{\Lambda}_1, \Lambda_1, \Lambda_3, \Lambda_4], & \text{for case 2,} \\ [\Lambda_1, \Lambda_2, \Lambda_4, \Lambda_3], & \text{for case 3,} \end{cases} \tag{59}$$

which satisfy

$$\Lambda_B^T D\Lambda_A = \langle v_1, v_2, v_3, v_4\rangle, \qquad \begin{cases} v_1 = v_2, \ v_3 = v_4, & \text{for case 1,} \\ v_1 = v_2, & \text{for case 2,} \\ v_3 = v_4, & \text{for case 3.} \end{cases} \tag{60}$$

In the above three cases, the general solution to Equation (57) can be given as

$$I(z) = \sum_{\alpha=1}^4 \lambda_\alpha(z)\Lambda_\alpha, \tag{61}$$

with

$$\lambda_\alpha(x_1) = \frac{e^{-\pi\varepsilon_\alpha} k'_\alpha X_\alpha(x_1)}{2\sqrt{2\pi}\cos(i\pi\varepsilon_\alpha)}. \tag{62}$$

In the above equation, for cases 1 and 2, the factors k'_1 and k'_2 are complex conjugates (that is, $k'_2 = \bar{k}'_1$), and k'_3 and k'_4 are real For case 3, k'_1, k'_2, k'_3, and k'_4 are real. $X_\alpha(z)$ is given by

$$X_\alpha(z) = \prod_{j=1}^{n} (z - a_j)^{-1/2+i\varepsilon_\alpha}(z - b_j)^{-1/2-i\varepsilon_\alpha}. \tag{63}$$

The arrangement of k'_i ensures that the strain and electric field are real (see Equation (69) below). Multiplying the two sides of (57) by $\boldsymbol{W} = \boldsymbol{\Lambda}_B^T \boldsymbol{D}$ with the elements $W_{\alpha j}$, with the aid of (61), we obtain:

$$[\lambda_\alpha(x_1)]^+ + e^{2\pi\varepsilon_\alpha}[\lambda_\alpha(x_1)]^- = \boldsymbol{W}^\alpha \boldsymbol{I}^0(x_1)/v_\alpha, \qquad \alpha = 1, 2, 3, 4, \tag{64}$$

where

$$\boldsymbol{I}^0(x_1) = \boldsymbol{\Omega} - \boldsymbol{u}_{,1}^\infty - \boldsymbol{u}_{a,1}(x_1), \tag{65}$$

and $\boldsymbol{W}^\alpha = [W_{\alpha 1}, W_{\alpha 2}, W_{\alpha 3}, W_{\alpha 4}]$. The solution to Equation (64) is given as

$$\lambda_\alpha(z) = \frac{X_\alpha(z)}{(1 + e^{2\pi\varepsilon_\alpha})v_\alpha} \left\{ \oint_\eta \frac{\boldsymbol{W}^\alpha \boldsymbol{\Omega}}{X_\alpha(\xi)(\xi - z)} d\xi - \boldsymbol{W}^\alpha \boldsymbol{u}_{,1}^\infty \left[\frac{1}{X_\alpha(z)} - x_\alpha(\infty) \right] \right.$$

$$- \frac{1}{i\pi} \sum_{j=1}^{4} W_{\alpha j} \sum_{k=1}^{4} N_{jk} d_k \left[\frac{1}{(z - z_{dk})X_\alpha(z)} - \frac{1}{(z - z_{dk})X_\alpha(z_{dk})} - 1 \right]$$

$$\left. + \frac{1}{i\pi} \sum_{j=1}^{4} W_{\alpha j} \sum_{k=1}^{4} \bar{N}_{jk} \bar{d}_k \left[\frac{1}{(z - \bar{z}_{dk})X_\alpha(z)} - \frac{1}{(z - \bar{z}_{dk})X_\alpha(\bar{z}_{dk})} - 1 \right] + P_\alpha^c(z) \right\}, \tag{66}$$

where

$$P_\alpha^c(z) = c_{\alpha n-1}^c z^{n-1} + \cdots + c_{\alpha 0}^c, \tag{67}$$

$$x_\alpha(\infty) = \prod_{j=1}^{n} [z - (a_j + b_j)/2 - i\varepsilon_\alpha(b_j - a_j)]. \tag{68}$$

The $4n$ constants $c_{\alpha k}^c$ ($\alpha = 1, 2, 3, 4$, $k = 0, 1, \ldots, n-1$) and n constants ω_j ($j = 1, 2, \ldots, n$) are obtained by substituting Equation (61) into Equations (35) and (36) with Equations (63) and (66)–(68). As a result, $\boldsymbol{F}_{kb}(z)$ can be found by using (26).

The generalized strains along the interface can be written as

$$\boldsymbol{u}_{,1}(x_1) = \frac{1}{\sqrt{2\pi}} [k'_1 X_1(x_1)\boldsymbol{\Lambda}_1 + k'_2 X_2(x_1)\boldsymbol{\Lambda}_2 + k'_3 X_3(x_1)\boldsymbol{\Lambda}_3 + k'_4 X_4(x_1)\boldsymbol{\Lambda}_4]. \tag{69}$$

The components $k'_1 X_1(x_1)$ and $k'_2 X_2(x_1)$ present the singularities of $r^{-1/2\mp i\varepsilon_\alpha}$, and $k'_3 X_3(x_1)$ and $k'_4 X_4(x_1)$ exhibit the singularities of $r^{-1/2\pm\kappa}$, at the interface a distance r ahead of the rigid conducting line tip. In cases 1 and 2, $k'_1 X_1(x_1)$ and $k'_2 X_2(x_1)$ are in the plane spanned by Re $[\boldsymbol{\Lambda}_1]$ and Im $[\boldsymbol{\Lambda}_1]$, and $k'_3 X_3(x_1)$

and $k'_4 X_4(x_1)$ are along the $\boldsymbol{\Lambda}_3$ and $\boldsymbol{\Lambda}_4$ directions, respectively. In case 3, $k'_i X_i(x_1)$ ($i = 1, 2, 3, 4$) are along the $\boldsymbol{\Lambda}_i$ directions. In case 1, the components are analogous to the corresponding tractions and charge for an impermeable interfacial crack in piezoelectric media, where $\varepsilon \neq 0$ and $\kappa \neq 0$ are assumed [Suo et al. 1992].

At the interface, the generalized stresses disturbed by rigid conducting lines are given by

$$\left[\sigma_{2j}(x_1), D_2(x_1)\right]^T = 2 \operatorname{Re}\left[\sum_{\alpha=1}^{4} \lambda_\alpha(x_1) \boldsymbol{B}_1 \boldsymbol{A}_1^{-1} \boldsymbol{\Lambda}_\alpha\right]. \tag{70}$$

At the tips of rigid conducting lines, the generalized stresses present oscillatory and nonsquare root singularities in case 1, oscillatory and square root singularities in case 2, and square root and nonsquare root singularities in case 3.

The generalized strain intensity factors at the right tip of the jth rigid conducting line are defined as

$$\begin{aligned}
\tilde{k}_\alpha &= \lim_{x_1 \to b_j} k'_\alpha \prod_{i=1}^{n} (x_1 - a_i)^{-1/2+i\varepsilon_\alpha} \prod_{i=1, i\neq j}^{n} (x_1 - b_i)^{-1/2-i\varepsilon_\alpha} \\
&= \lim_{x_1 \to b_j} 2\sqrt{2\pi} \cos(i\pi\varepsilon_\alpha) e^{\pi\varepsilon_\alpha} (x_1 - b_j)^{1/2+i\varepsilon_\alpha} \lambda_\alpha(x_1),
\end{aligned} \tag{71}$$

where $\tilde{k}_1$ and $\tilde{k}_2$ are complex conjugates, and $\tilde{k}_3$ and $\tilde{k}_4$ are real for cases 1 and 2. All $\tilde{k}_i$ are real for case 3.

At the interface a distance r ahead of the jth rigid conducting line tip, the generalized displacements are

$$\boldsymbol{u}(r) = \sqrt{\frac{r}{2\pi}} \sum_{\alpha=1}^{4} \frac{2}{1 - i2\varepsilon_\alpha} \tilde{k}_\alpha r^{-i\varepsilon_\alpha} \boldsymbol{\Lambda}_\alpha. \tag{72}$$

The generalized stress jumps at the interface a distance r behind the jth rigid conducting line tip are

$$\Delta\boldsymbol{\Phi}_{,1}(r) = \boldsymbol{D}\sqrt{\frac{1}{2\pi r}} \sum_{\alpha=1}^{4} \frac{1}{\cos(i\pi\varepsilon_\alpha)} \tilde{k}_\alpha r^{-i\varepsilon_\alpha} \boldsymbol{\Lambda}_\alpha. \tag{73}$$

It is worth noting that the structure of the generalized displacements in Equation (72) is the same as that of the generalized stresses ahead of an impermeable crack tip, and the structure of the generalized stress jumps in Equation (73) is the same as that of the generalized displacement jumps behind the crack tip [Suo et al. 1992].

By substituting Equations (72) and (73) into (54), the jth rigid line extension force is obtained as

$$G = \begin{cases}
-\dfrac{v_1}{2\cosh^2 \pi\varepsilon}|\tilde{k}_1|^2 - \dfrac{v_3}{2\cos^2 \pi\kappa}\tilde{k}_3\tilde{k}_4, & \text{for case 1,} \\[3mm]
-\dfrac{v_1}{2\cosh^2 \pi\varepsilon}|\tilde{k}_1|^2 - \dfrac{v_3}{4}\tilde{k}_3^2 - \dfrac{v_4}{4}\tilde{k}_4^2, & \text{for case 2,} \\[3mm]
-\dfrac{v_1}{4}\tilde{k}_1^2 - \dfrac{v_2}{4}\tilde{k}_2^2 - \dfrac{v_3}{2\cos^2 \pi\kappa}\tilde{k}_3\tilde{k}_4, & \text{for case 3.}
\end{cases} \tag{74}$$

4.4. *Rigid dielectric lines: the fields of oscillatory and square root singularities.* For complex Y, Equations (5), (6), (7), (27), and (39) lead to

$$\hat{I}^+(x_1) + \bar{\Lambda}^{-1}\hat{Y}\hat{I}^-(x_1) = \hat{\Omega} - \hat{u}_{,1}^\infty - \hat{u}_{a,1}(x_1). \tag{75}$$

Similarly, the eigenvalues of $\bar{\Lambda}^{-1}\hat{Y}$ are assumed to be the form $e^{2\pi\varepsilon_\alpha}$. One has

$$\varepsilon_{1,2} = \pm\varepsilon, \qquad \varepsilon_3 = 0, \tag{76}$$

where

$$\varepsilon = \frac{1}{2\pi}\ln\frac{1+\eta}{1-\eta}, \qquad \eta = \sqrt{-\frac{1}{2}\operatorname{tr}[(\hat{D}^{-1}\hat{U})^2]}, \qquad \hat{D} = \operatorname{Re}[\hat{Y}], \qquad \hat{U} = \operatorname{Im}[\hat{Y}]. \tag{77}$$

The associated eigenvectors Λ_1 and Λ_2 are complex conjugates, that is, $\Lambda_2 = \bar{\Lambda}_1$, and Λ_3 is real. We define

$$\Lambda_A = [\Lambda_1, \bar{\Lambda}_1, \Lambda_3], \qquad \Lambda_B = [\bar{\Lambda}_1, \Lambda_1, \Lambda_3], \tag{78}$$

which satisfy

$$\Lambda_B^T\hat{D}\Lambda_A = \langle v_1, v_2, v_3 \rangle, \qquad v_1 = v_2. \tag{79}$$

The general solution of Equation (75) can be given as

$$\hat{I}(z) = \sum_{\alpha=1}^{3} \lambda_\alpha(z)\Lambda_\alpha, \tag{80}$$

where $\lambda_\alpha(z)$ is evaluated by Equation (62), with the factors k_1' and k_2' being complex conjugates, and k_3' being real. A similar procedure to that adopted in the preceding section permits us to obtain

$$
\begin{aligned}
\lambda_\alpha(z) = &\frac{X_\alpha(z)}{(1+e^{2\pi\varepsilon_\alpha})v_\alpha}\left\{ \oint_\eta \frac{\hat{W}^\alpha\hat{\Omega}}{X_\alpha(\xi)(\xi-z)}d\xi - \hat{W}^\alpha\hat{u}_{,1}^\infty\left[\frac{1}{X_\alpha(z)} - x_\alpha(\infty)\right] \right. \\
&- \frac{1}{i\pi}\sum_{j=1}^{3}\hat{W}_{\alpha j}\sum_{k=1}^{4}N_{jk}d_k\left[\frac{1}{(z-z_{dk})X_\alpha(z)} - \frac{1}{(z-z_{dk})X_\alpha(z_{dk})} - 1\right] \\
&\left. + \frac{1}{i\pi}\sum_{j=1}^{3}\hat{W}_{\alpha j}\sum_{k=1}^{4}\bar{N}_{jk}\bar{d}_k\left[\frac{1}{(z-\bar{z}_{dk})X_\alpha(z)} - \frac{1}{(z-\bar{z}_{dk})X_\alpha(\bar{z}_{dk})} - 1\right] + P_\alpha^d(z) \right\}, \tag{81}
\end{aligned}
$$

where $\hat{W}^\alpha$ denotes the first (α) row of the matrix $\hat{W} = \hat{\Lambda}_B^T\hat{D}$ with the elements $\hat{W}_{ij}$, and

$$P_\alpha^d(z) = c_{\alpha n-1}^d z^{n-1} + \cdots + c_{\alpha 0}^d. \tag{82}$$

Substituting Equation (80) into (44) and (45), with Equations (63), (68), (81), and (82), we find the $3n$ constants $c_{\alpha k}^d$ ($\alpha = 1, 2, 3, \ k = 0, 1, \ldots, n-1$) and the n constants ω_j ($j = 1, 2, \ldots, n$). The functions $F_{kb}(z)$ are obtained through (26).

The strains along the interface can be written as

$$\hat{u}_{,1}(x_1) = \frac{1}{\sqrt{2\pi}} \big[k_1' X_1(x_1) \boldsymbol{\Lambda}_1 + \bar{k}_1' \bar{X}_1(x_1) \bar{\boldsymbol{\Lambda}}_1 + k_3' X_3(x_1) \boldsymbol{\Lambda}_3 \big]. \tag{83}$$

It is noted that the strains can be decomposed into two components: one is in the plane spanned by $\mathrm{Re}\,[\boldsymbol{\Lambda}_1]$ and $\mathrm{Im}\,[\boldsymbol{\Lambda}_1]$, and the other is along the $\boldsymbol{\Lambda}_3$ direction, in analogy to the tractions for a crack in anisotropic elastic media [Suo 1990]. At the jth rigid dielectric line tip, the strains present oscillatory and square root singularities. The strain intensity factors $\tilde{k}_\alpha$ ($\alpha = 1, 2, 3$) defined in Equation (71) for the conducting case are used here to characterize these singularities together with (81). The electric field at the bonded interface is given by

$$E_1(x_1) = 2\,\mathrm{Re}\,[\boldsymbol{e}^T \hat{\boldsymbol{I}}(x)], \tag{84}$$

where $\boldsymbol{e} = \big[-Y_{41}/Y_{44}, -Y_{42}/Y_{44}, -Y_{43}/Y_{44} \big]^T$. Equation (84) implies that the tip electric field also exhibits oscillatory and square root singularities.

Along the interface, the generalized stresses disturbed by the rigid dielectric lines are obtained as

$$\big[\sigma_{2j}(x_1), D_2(x_1) \big]^T = 2\,\mathrm{Re}\,\Bigg[\boldsymbol{B}_1 \boldsymbol{A}_1^{-1}(\hat{\boldsymbol{I}} - \boldsymbol{E}) \sum_{\alpha=1}^{3} \lambda_\alpha(x_1) \boldsymbol{\Lambda}_\alpha \Bigg]. \tag{85}$$

It should be noted that the near-tip stress and electric displacement fields present oscillatory and square root singularities, similar to the fields near the tips of a permeable interfacial crack in piezoelectric media [Beom 2003].

At a distance r ahead of the jth rigid dielectric line tip, the displacements are

$$\hat{u}(r) = \sqrt{\frac{r}{2\pi}} \sum_{\alpha=1}^{3} \frac{2}{1 - i2\varepsilon_\alpha} \tilde{k}_\alpha r^{-i\varepsilon_\alpha} \boldsymbol{\Lambda}_\alpha. \tag{86}$$

The stress jumps at a distance r behind the jth rigid dielectric line tip are

$$\big[\Delta\sigma_{21}(r), \Delta\sigma_{22}(r), \Delta\sigma_{23}(r) \big]^T = \hat{\boldsymbol{D}} \sqrt{\frac{1}{2\pi r}} \sum_{\alpha=1}^{3} \frac{1}{\cos(i\pi\varepsilon_\alpha)} \tilde{k}_\alpha r^{-i\varepsilon_\alpha} \boldsymbol{\Lambda}_\alpha. \tag{87}$$

By substituting Equations (86) and (87) into Equation (54), the jth rigid line extension force is obtained as

$$G = -\frac{v_1}{2\cosh^2 \pi\varepsilon} |\tilde{k}_1|^2 - \frac{v_3}{4} \tilde{k}_3^2. \tag{88}$$

5. Near tip fields around a single rigid line with a real Y

In this section we consider a single interfacial rigid line of length $2a$ centered along the x_1 axis for the case that Y is real. The rotation of the rigid line is assumed to be ω. One has

$$\boldsymbol{\Omega} = \big[0, \omega, 0, 0 \big]^T, \tag{89}$$

$$\hat{\boldsymbol{\Omega}} = \big[0, \omega, 0 \big]^T, \tag{90}$$

$$X(z) = (z+a)^{-1/2}(z-a)^{-1/2}, \qquad x(\infty) = z.$$

5.1. *A single rigid conducting line: the fields of a square root singularity.* In this case, Equation (31) becomes

$$I(z) = \frac{1}{2}(\boldsymbol{\Omega} - \boldsymbol{u}_{,1}^{\infty})\left[1 - \frac{z}{\sqrt{z^2 - a^2}}\right] - \frac{1}{2\pi i}\boldsymbol{N}\left\langle \frac{1}{z_\alpha - z_{d\alpha}}\left(1 - \sqrt{\frac{z_{d\alpha}^2 - a^2}{z_\alpha^2 - a^2}}\right) - \frac{1}{\sqrt{z_\alpha^2 - a^2}}\right\rangle \boldsymbol{d}$$

$$+ \frac{1}{2\pi i}\bar{\boldsymbol{N}}\left\langle \frac{1}{z_\alpha - z_{d\alpha}}\left(1 - \sqrt{\frac{z_{d\alpha}^2 - a^2}{z_\alpha^2 - a^2}}\right) - \frac{1}{\sqrt{z_\alpha^2 - a^2}}\right\rangle \bar{\boldsymbol{d}} + \frac{z}{2\sqrt{z^2 - a^2}}\boldsymbol{c}_0^a(z)\bigg\}. \quad (91)$$

Substituting Equation (91) into (35) and (36), and applying the residue theorem, we have

$$\boldsymbol{c}_0^a = 0, \tag{92}$$

$$\omega = \frac{1}{Y_{22}}\left\{\boldsymbol{Y}^{(2)}\boldsymbol{u}_{,1}^{\infty} + \frac{4}{\pi a^2}\,\mathrm{Im}\left[\boldsymbol{Y}^{(2)}\boldsymbol{N}\left\langle\sqrt{z_{d\alpha}^2 - a^2} - z_{d\alpha}\right\rangle\boldsymbol{d}\right]\right\}. \tag{93}$$

Substituting Equation (91) into (26) with Equations (92) and (93), using Equations (19)–(22), and neglecting constants, one has

$$\boldsymbol{F}_1(z) = \frac{1}{2\pi i}\boldsymbol{A}_1^{-1}\left\{\boldsymbol{A}_1\left\langle\frac{1}{z_\alpha - z_{d\alpha}}\right\rangle\boldsymbol{d} - \boldsymbol{N}\left\langle\frac{1}{z_\alpha - z_{d\alpha}}\left[1 - \sqrt{\frac{z_{d\alpha}^2 - a^2}{z_\alpha^2 - a^2}}\right] - \frac{1}{\sqrt{z_\alpha^2 - a^2}}\right\rangle\boldsymbol{d}\right.$$

$$\left. + \bar{\boldsymbol{A}}_1\left\langle\frac{1}{z_\alpha - \bar{z}_{d\alpha}}\right\rangle\bar{\boldsymbol{d}} - \bar{\boldsymbol{N}}\left\langle\frac{1}{z_\alpha - \bar{z}_{d\alpha}}\left[1 + \sqrt{\frac{\bar{z}_{d\alpha}^2 - a^2}{z_\alpha^2 - a^2}}\right] + \frac{1}{\sqrt{z_\alpha^2 - a^2}}\right\rangle\bar{\boldsymbol{d}} + (\boldsymbol{u}_{,1}^{\infty} - \boldsymbol{\Omega})\frac{i\pi z}{\sqrt{z^2 - a^2}}\right\}, \quad (94)$$

$$\boldsymbol{F}_2(z) = \frac{1}{2\pi i}\boldsymbol{A}_2^{-1}\left\{\boldsymbol{N}\left\langle\frac{1}{z_\alpha - z_{d\alpha}}\left[1 + \sqrt{\frac{z_{d\alpha}^2 - a^2}{z_\alpha^2 - a^2}}\right] + \frac{1}{\sqrt{z_\alpha^2 - a^2}}\right\rangle\boldsymbol{d}\right.$$

$$\left. + \bar{\boldsymbol{N}}\left\langle\frac{1}{z_\alpha - \bar{z}_{d\alpha}}\left[1 - \sqrt{\frac{\bar{z}_{d\alpha}^2 - a^2}{z_\alpha^2 - a^2}}\right] - \frac{1}{\sqrt{z_\alpha^2 - a^2}}\right\rangle\bar{\boldsymbol{d}} + (\boldsymbol{u}_{,1}^{\infty} - \boldsymbol{\Omega})\frac{i\pi z}{\sqrt{z^2 - a^2}}\right\}. \quad (95)$$

Substitution of Equations (94) and (95) into (2) yields the complete stress and electric displacement field solutions in s_1 and s_2, respectively.

By substituting Equation (91) into Equations (46) with (93), the generalized strain intensity factors at the right tip of the rigid conducting line are obtained as

$$\boldsymbol{k} = \sqrt{\pi a}(\boldsymbol{u}_{,1}^{\infty} - \boldsymbol{\Omega}) + \frac{2}{\sqrt{\pi a}}\,\mathrm{Im}\left[\boldsymbol{N}\left\langle 1 - \sqrt{\frac{z_{d\alpha} + a}{z_{d\alpha} - a}}\right\rangle\boldsymbol{d}\right]. \tag{96}$$

Substituting Equation (91) into (47), one has the generalized stress intensity factors at the right tip of the rigid conducting line $\boldsymbol{K} = \boldsymbol{S}_1^T\boldsymbol{H}_1^{-1}\boldsymbol{k} = \boldsymbol{S}_2^T\boldsymbol{H}_2^{-1}\boldsymbol{k}$, where $\boldsymbol{S}_1^T\boldsymbol{H}_1^{-1} = \boldsymbol{S}_2^T\boldsymbol{H}_2^{-1}$ for real $\boldsymbol{Y}$.

Substituting Equation (96) into (55) yields

$$G = -\frac{\pi a}{4}(\boldsymbol{u}_{,1}^\infty - \boldsymbol{\Omega})^T \boldsymbol{Y}(\boldsymbol{\Omega} - \boldsymbol{u}_{,1}^\infty) - (\boldsymbol{u}_{,1}^\infty - \boldsymbol{\Omega})^T \boldsymbol{Y} \operatorname{Im}\left[\boldsymbol{N}\left\langle 1 - \sqrt{\frac{z_{d\alpha}+a}{z_{d\alpha}-a}}\right\rangle \boldsymbol{d}\right]$$

$$-\frac{1}{\pi a}\operatorname{Im}\left[\boldsymbol{d}^T\left\langle 1 - \sqrt{\frac{z_{d\alpha}+a}{z_{d\alpha}-a}}\right\rangle \boldsymbol{N}^T\right]\boldsymbol{Y}\operatorname{Im}\left[\boldsymbol{N}\left\langle 1 - \sqrt{\frac{z_{d\alpha}+a}{z_{d\alpha}-a}}\right\rangle \boldsymbol{d}\right]. \quad (97)$$

5.2. *A single rigid dielectric line: the fields of a square root singularity.* In this case, Equation (42) reads

$$\hat{\boldsymbol{I}}(z) = (\hat{\boldsymbol{\Omega}} - \hat{\boldsymbol{u}}_{,1}^\infty)\left[\frac{1}{2} - \frac{z}{2\sqrt{z^2-a^2}}\right] - \frac{1}{2\pi i}\hat{\boldsymbol{N}}\left\langle \frac{1}{z_\alpha - z_{d\alpha}}\left[1 - \sqrt{\frac{z_{d\alpha}^2-a^2}{z_\alpha^2-a^2}}\right] - \frac{1}{\sqrt{z_\alpha^2-a^2}}\right\rangle \boldsymbol{d}$$

$$+ \frac{1}{2\pi i}\bar{\hat{\boldsymbol{N}}}\left\langle \frac{1}{z_\alpha - \bar{z}_{d\alpha}}\left[1 - \sqrt{\frac{\bar{z}_{d\alpha}^2-a^2}{z_\alpha^2-a^2}}\right] - \frac{1}{\sqrt{z_\alpha^2-a^2}}\right\rangle \bar{\boldsymbol{d}} + \frac{z}{2\sqrt{z^2-a^2}}\boldsymbol{c}_0^b. \quad (98)$$

Substituting Equation (98) into Equations (44) and (45), and applying the residue theorem, we obtain

$$\boldsymbol{c}_0^b = \boldsymbol{0}, \quad (99)$$

$$\omega = \frac{1}{\hat{Y}_{2j}}\left\{\sum_{j=1}^3 \hat{Y}_{2j}u_{j,1}^\infty + \frac{4}{\pi a^2}\operatorname{Im}\left[\hat{\boldsymbol{Y}}\hat{\boldsymbol{N}}\left\langle \sqrt{z_{d\alpha}^2-a^2} - z_{d\alpha}\right\rangle \boldsymbol{d}\right]\right\}. \quad (100)$$

Substituting Equation (98) into (39), using Equations (19)–(22), and (26), and neglecting constants, we have

$$\boldsymbol{F}_1(z) = \boldsymbol{A}_1^{-1}\left\{\frac{1}{2\pi i}\boldsymbol{A}_1\left\langle \frac{1}{z_\alpha - z_{d\alpha}}\right\rangle \boldsymbol{d} - \frac{1}{2\pi i}(2\bar{\boldsymbol{N}} - \bar{\boldsymbol{A}}_1)\left\langle \frac{1}{z_\alpha - \bar{z}_{d\alpha}}\right\rangle \bar{\boldsymbol{d}}\right\}$$

$$-\frac{1}{2\pi i}\boldsymbol{A}_1^{-1}(\hat{\boldsymbol{I}} - \boldsymbol{E})\left\{\hat{\boldsymbol{N}}\left\langle \frac{1}{z_\alpha - z_{d\alpha}}\left[1 - \sqrt{\frac{z_{d\alpha}^2-a^2}{z_\alpha^2-a^2}}\right] - \frac{1}{\sqrt{z_\alpha^2-a^2}}\right\rangle \boldsymbol{d}\right. \quad (101)$$

$$\left. - \bar{\hat{\boldsymbol{N}}}\left\langle \frac{1}{z_\alpha - \bar{z}_{d\alpha}}\left[1 - \sqrt{\frac{\bar{z}_{d\alpha}^2-a^2}{z_\alpha^2-a^2}}\right] - \frac{1}{\sqrt{z_\alpha^2-a^2}}\right\rangle \bar{\boldsymbol{d}} + (\hat{\boldsymbol{\Omega}} - \hat{\boldsymbol{u}}_{,1}^\infty)\frac{i\pi z}{\sqrt{z^2-a^2}}\right\},$$

$$\boldsymbol{F}_2(z) = \boldsymbol{A}_2^{-1}\left\{\frac{1}{2\pi i}\boldsymbol{N}\left\langle \frac{2}{z_\alpha - z_{d\alpha}}\right\rangle \boldsymbol{d}\right.$$

$$+ (\hat{\boldsymbol{I}} - \boldsymbol{E})\left[-\frac{1}{2\pi i}\hat{\boldsymbol{N}}\left\langle \frac{1}{z_\alpha - z_{d\alpha}}\left[1 - \sqrt{\frac{z_{d\alpha}^2-a^2}{z_\alpha^2-a^2}}\right] - \frac{1}{\sqrt{z_\alpha^2-a^2}}\right\rangle \boldsymbol{d}\right. \quad (102)$$

$$\left.\left. + \frac{1}{2\pi i}\bar{\hat{\boldsymbol{N}}}\left\langle \frac{1}{z_\alpha - \bar{z}_{d\alpha}}\left[1 - \sqrt{\frac{\bar{z}_{d\alpha}^2-a^2}{z_\alpha^2-a^2}}\right] - \frac{1}{\sqrt{z_\alpha^2-a^2}}\right\rangle \bar{\boldsymbol{d}} - (\hat{\boldsymbol{\Omega}} - \hat{\boldsymbol{u}}_{,1}^\infty)\frac{z}{2\sqrt{z^2-a^2}}\right]\right\}.$$

Substituting Equations (101) and (102) into (2) leads to the complete stress and electric displacement field solutions in s_1 and s_2, respectively.

Substituting Equation (98) into (49) with (100), and using Equation (48), we obtain the generalized strain intensity factors at the right tip of the rigid dielectric line as

$$k = \sqrt{\pi a}(\hat{I} - E)(\hat{u}_{,1}^\infty - \hat{\Omega}) + \frac{2}{\sqrt{\pi a}}(\hat{I} - E)\,\mathrm{Im}\left[\hat{N}\left\langle 1 - \sqrt{\frac{z_{d\alpha} + a}{z_{d\alpha} - a}}\right\rangle d\right]. \tag{103}$$

Substituting Equation (98) into (47) with (100), one finds the generalized stress intensity factors at the right tip of the rigid dielectric line as

$$K = S_1^T H_1^{-1} k = S_2^T H_2^{-1} k. \tag{104}$$

Substituting Equation (103) into (56) leads to

$$G = -\frac{\pi a}{4}(\hat{u}_{,1}^\infty - \hat{\Omega})^T \hat{Y}(\hat{u}_{,1}^\infty - \hat{\Omega}) - (\hat{u}_{,1}^\infty - \hat{\Omega})^T \hat{Y}\,\mathrm{Im}\left[\hat{N}\left\langle 1 - \sqrt{\frac{z_{d\alpha} + a}{z_{d\alpha} - a}}\right\rangle d\right]$$
$$- \frac{1}{\pi a}\,\mathrm{Im}\left[d^T\left\langle 1 - \sqrt{\frac{z_{d\alpha} + a}{z_{d\alpha} - a}}\right\rangle \hat{N}^T\right]\hat{Y}\,\mathrm{Im}\left[\hat{N}\left\langle 1 - \sqrt{\frac{z_{d\alpha} + a}{z_{d\alpha} - a}}\right\rangle d\right]. \tag{105}$$

It is observed that the electric field applied at infinity cannot induce the rotation of the interfacial rigid dielectric line, and makes no contribution to the singularities of the stress and electric displacement fields at the tips of the interfacial rigid dielectric line in the two half-infinite planes.

6. Near-tip fields around a single rigid line with a complex Y

In this section, let us consider a rigid line of length $2a$ centered along the x_1 axis, when Y is complex. The rotation of the rigid line is assumed to be ω. Equations (30) and (41) become Equations (89) and (90), respectively. Equations (63) and (68) become

$$X_\alpha(z) = (z + a)^{-1/2 + i\varepsilon_\alpha}(z - a)^{-1/2 - i\varepsilon_\alpha}, \tag{106}$$
$$x_\alpha(\infty) = z - i2a\varepsilon_\alpha, \tag{107}$$

respectively. For convenience, we define

$$q_1(z, \alpha) = \frac{z - i2a\varepsilon_\alpha}{\sqrt{z^2 - a^2}}\left[\frac{z + a}{z - a}\right]^{i\varepsilon_\alpha}, \tag{108}$$

$$q_2(z, z_{d\beta}, \alpha) = \frac{1}{z - z_{d\beta}}\left\{1 - \sqrt{\frac{z_{d\beta}^2 - a^2}{z^2 - a^2}}\left[\frac{z + a}{z - a}\right]^{i\varepsilon_\alpha}\left[\frac{z_{d\beta} - a}{z_{d\beta} + a}\right]^{i\varepsilon_\alpha}\right\} - \frac{1}{\sqrt{z^2 - a^2}}\left[\frac{z + a}{z - a}\right]^{i\varepsilon_\alpha}. \tag{109}$$

6.1. A single rigid conducting line: the fields of square root, nonsquare root and oscillatory singularities. Substituting Equation (66) into Equations (35), and (36), with Equations (67) ($n = 1$), (89), (106),

and (107), and applying the residue theorem, we have

$$\lambda_\alpha(z) = (W^\alpha u_{,1}^\infty - W_{\alpha 2}\omega)q_1(z, \alpha)$$
$$- \frac{1}{i\pi} \sum_{j=1}^4 W_{\alpha j} \left[\sum_{\beta=1}^4 N_{j\beta} d_\beta q_2(z, z_{d\beta}, \alpha) - \sum_{k=1}^4 \bar{N}_{j\beta} \bar{d}_\beta q_2(z, \bar{z}_{d\beta}, \alpha) \right], \quad (110)$$

$$\omega = \rho_1 \sum_{k=1}^4 \upsilon_k \left\{ \sum_{j=1}^4 \frac{1}{i\pi a^2} W_{kj} \left\{ \sum_{r=1}^4 N_{jr} d_r \left[i2a\varepsilon_k - z_{dr} + (z_{dr} + a)^{1/2-i\varepsilon_k}(z_{dr} - a)^{1/2+i\varepsilon_k} \right] \right.\right.$$
$$\left.\left. - \sum_{r=1}^4 \bar{N}_{jr} \bar{d}_r \left[i2a\varepsilon_k - \bar{z}_{dr} + (\bar{z}_{dr} + a)^{1/2-i\varepsilon_k}(\bar{z}_{dr} - a)^{1/2+i\varepsilon_k} \right] \right\} + W^k u_{j,1}^\infty (1/2 + 2\varepsilon_k^2) \right\}, \quad (111)$$

where

$$\rho_1 = 1 \bigg/ \sum_{k=1}^4 \upsilon_k W_{k2}(1/2 + 2\varepsilon_k^2), \qquad \upsilon_k = \frac{\Xi_k}{(1 + e^{2\pi\varepsilon_k})v_k}, \quad (112)$$

with Ξ_k being the elements of the 1×4 matrix $\Xi = Y^{(2)}\Lambda_A$.

Substituting Equation (110) into (61) with (111), and using Equations (19)–(22), and (26), we find

$$F_1(z) = \frac{1}{2\pi i} \left[\left\langle \frac{1}{z_\alpha - z_{d\alpha}} \right\rangle d - A_1^{-1}(2\bar{N} - \bar{A}_1)\left\langle \frac{1}{z_\alpha - \bar{z}_{d\alpha}} \right\rangle \bar{d} \right] + A_1^{-1} \sum_{\alpha=1}^4 \frac{\lambda_\alpha \Lambda_\alpha}{(1 + e^{2\pi\varepsilon_\alpha})v_\alpha}, \quad (113)$$

$$F_2(z) = \frac{1}{\pi i} A_2^{-1} N \left\langle \frac{1}{z_\alpha - z_{d\alpha}} \right\rangle d + A_2^{-1}\bar{Y}^{-1}Y \sum_{\alpha=1}^4 \frac{\lambda_\alpha \Lambda_\alpha}{(1 + e^{2\pi\varepsilon_\alpha})v_\alpha}. \quad (114)$$

Substitution of the above equations into Equation (2) yields the complete stress and electric displacement field solutions in s_1 and s_2.

By substituting Equation (110) into (71), the generalized strain intensity factors at the right tip of the rigid conducting line are obtained as

$$\tilde{k}_\alpha = \frac{(2a)^{i\varepsilon_\alpha}}{v_\alpha} \left\{ \frac{1}{i\sqrt{\pi a}} \sum_{j=1}^4 W_{\alpha j} \left\{ \sum_{k=1}^4 N_{jk} d_k \left[1 - \sqrt{\frac{z_{dk} + a}{z_{dk} - a}} \left(\frac{z_{dk} - a}{z_{dk} + a} \right)^{i\varepsilon_\alpha} \right] \right.\right.$$
$$\left.\left. - \sum_{k=1}^4 \bar{N}_{jk} \bar{d}_k \left[1 - \sqrt{\frac{\bar{z}_{dk} + a}{\bar{z}_{dk} - a}} \left(\frac{\bar{z}_{dk} - a}{\bar{z}_{dk} + a} \right)^{i\varepsilon_\alpha} \right] \right\} + \sqrt{\pi a} W^\alpha (u_{,1}^\infty - \Omega)(1 - i2\varepsilon_\alpha) \right\}. \quad (115)$$

The rigid line extension force can be obtained by substituting Equation (115) into (74). This solution procedure is not given in detail here.

6.2. *A single rigid dielectric line: the fields of square root and oscillatory singularities.* Substituting Equation (80) into (44), and (45) with Equations (81) ($n = 1$), (90), (106), and (107), and applying the

residue theorem, we have

$$
\lambda_\alpha(z) = (\hat{\boldsymbol{W}}^\alpha \hat{\boldsymbol{u}}_{,1}^\infty - \hat{W}_{\alpha 2}\omega)q_1(z, \alpha)
$$
$$
- \frac{1}{i\pi} \sum_{j=1}^{3} \hat{W}_{\alpha j} \left[\sum_{\beta=1}^{4} N_{j\beta} d_\beta q_2(z, z_{d\beta}, \alpha) - \sum_{k=1}^{4} \bar{N}_{j\beta} \bar{d}_\beta q_2(z, \bar{z}_{d\beta}, \alpha) \right], \quad (116)
$$

$$
\omega = \rho_2 \sum_{k=1}^{3} \vartheta_k \left\{ \frac{1}{i\pi a^2} \sum_{j=1}^{3} \hat{W}_{kj} \left\{ \sum_{r=1}^{4} N_{jr} d_r \left[i2a\varepsilon_k - z_{dr} + (z_{dr} + a)^{1/2 - i\varepsilon_k}(z_{dr} - a)^{1/2 + i\varepsilon_k} \right] \right. \right.
$$
$$
\left. \left. - \sum_{r=1}^{4} \bar{N}_{jr} \bar{d}_r \left[i2a\varepsilon_k - \bar{z}_{dr} + (\bar{z}_{dr} + a)^{1/2 - i\varepsilon_k}(\bar{z}_{dr} - a)^{1/2 + i\varepsilon_k} \right] \right\} + \sum_{j=1}^{3} \hat{W}_{kj} \hat{u}_{j,1}^\infty (1/2 + 2\varepsilon_k^2) \right\}, \quad (117)
$$

where

$$
\rho_2 = \frac{1}{\displaystyle\sum_{k=1}^{3} \vartheta_k \hat{W}_{k2}(1/2 + 2\varepsilon_k^2)}, \qquad \vartheta_k = \frac{Q_k}{(1 + e^{2\pi\varepsilon_k})v_k}, \quad (118)
$$

with Q_k being the elements of the 1×3 matrix $\boldsymbol{Q} = \hat{\boldsymbol{Y}}^{(2)}\boldsymbol{\Lambda}_A$.

Substituting Equation (116) into (80) with (117), and using Equations (19)–(22), (26), and (39), we find

$$
\boldsymbol{F}_1(z) = \frac{1}{2\pi i} \left[\left\langle \frac{1}{z_\alpha - z_{d\alpha}} \right\rangle \boldsymbol{d} - \boldsymbol{A}_1^{-1}(2\bar{\boldsymbol{N}} - \bar{\boldsymbol{A}}_1) \left\langle \frac{1}{z_\alpha - \bar{z}_{d\alpha}} \right\rangle \bar{\boldsymbol{d}} \right] + \boldsymbol{A}_1^{-1}(\hat{\boldsymbol{I}} - \boldsymbol{E}) \sum_{\alpha=1}^{3} \frac{\lambda_\alpha \boldsymbol{\Lambda}_\alpha}{(1 + e^{2\pi\varepsilon_\alpha})v_\alpha}, \quad (119)
$$

$$
\boldsymbol{F}_2(z) = \frac{1}{\pi i} \boldsymbol{A}_2^{-1} \boldsymbol{N} \left\langle \frac{1}{z_\alpha - z_{d\alpha}} \right\rangle \boldsymbol{d} + \boldsymbol{A}_2^{-1} \bar{\boldsymbol{Y}}^{-1} \boldsymbol{Y}(\hat{\boldsymbol{I}} - \boldsymbol{E}) \sum_{\alpha=1}^{3} \frac{\lambda_\alpha \boldsymbol{\Lambda}_\alpha}{(1 + e^{2\pi\varepsilon_\alpha})v_\alpha}. \quad (120)
$$

Substitution of the above equations into Equation (2) yields the complete stress and electric displacement field solution in s_1 and s_2.

By substituting Equation (116) into (71), the strain intensity factors at the right tip of the rigid dielectric line are obtained as

$$
\tilde{k}_\alpha = \frac{(2a)^{i\varepsilon_\alpha}}{v_\alpha} \left\{ \frac{1}{i\sqrt{\pi a}} \sum_{j=1}^{3} \hat{W}_{\alpha j} \left\{ \sum_{k=1}^{4} N_{jk} d_k \left[1 - \sqrt{\frac{z_{dk} + a}{z_{dk} - a}} \left(\frac{z_{dk} - a}{z_{dk} + a} \right)^{i\varepsilon_\alpha} \right] \right. \right.
$$
$$
\left. - \sum_{k=1}^{4} \bar{N}_{jk} \bar{d}_k \left[1 - \sqrt{\frac{\bar{z}_{dk} + a}{\bar{z}_{dk} - a}} \left(\frac{\bar{z}_{dk} - a}{\bar{z}_{dk} + a} \right)^{i\varepsilon_\alpha} \right] \right]
$$
$$
\left. + \sqrt{\pi a}\,\hat{\boldsymbol{W}}^\alpha (\hat{\boldsymbol{u}}_{,1}^\infty - \hat{\boldsymbol{\Omega}})(1 - i2\varepsilon_\alpha) \right\}, \quad (121)
$$

for $\alpha = 1, 2, 3$. The rigid line extension force can be obtained by substituting Equation (121) into (88).

Similar to the case in which Y is real, the electric field applied at infinity does not affect either the rotation of the single interfacial rigid dielectric line, or the stress and electric displacement fields in the two half-infinite planes with the single interfacial rigid dielectric line.

7. Image force on the piezoelectric dislocation

The image forces in the x and y directions on the piezoelectric dislocation are obtained from the generalized Peach–Koehler formula [Pak 1990b] as

$$F_x = \sigma_{i2}^d b_i = \boldsymbol{b}^T \boldsymbol{\Phi}_{,1}^d, \qquad F_y = -\sigma_{i1}^d b_i = \boldsymbol{b}^T \boldsymbol{\Phi}_{,2}^d,$$

where σ_{i2}^d (or $\boldsymbol{\Phi}_{,1}^d$) and σ_{i1}^d (or $-\boldsymbol{\Phi}_{,2}^d$) are the generalized stresses obtained by subtracting the fields generated by the piezoelectric dislocation with $z \to z_d$. Here we consider the case of a single rigid line of length $2a$ centered along the interface of two piezoelectric media in the absence of far-field loads.

7.1. *A single rigid conducting line.* For the case in which Y is real, we obtain, from Equations (2), (3), and (94):

$$\boldsymbol{\Phi}_{,1}^d = \frac{1}{\pi} \operatorname{Im}\left[\boldsymbol{B}_1 \boldsymbol{A}_1^{-1} \bar{\boldsymbol{A}}_1 \langle g_1(z_{d\alpha})\rangle \bar{\boldsymbol{B}}_1^T \boldsymbol{b} - \boldsymbol{B}_1 \boldsymbol{A}_1^{-1} \boldsymbol{N} \langle g_2(z_{d\alpha})\rangle \boldsymbol{B}_1^T \boldsymbol{b} \right.$$
$$\left. - \boldsymbol{B}_1 \boldsymbol{A}_1^{-1} \bar{\boldsymbol{N}} \langle g_3(z_{d\alpha})\rangle \bar{\boldsymbol{B}}_1^T \boldsymbol{b}\right] - \operatorname{Re}\left[\boldsymbol{B}_1 \boldsymbol{A}_1^{-1} \boldsymbol{\Omega} g_4(z_d)\right],$$

$$\boldsymbol{\Phi}_{,2}^d = \frac{1}{\pi} \operatorname{Im}\left[\boldsymbol{B}_1 \boldsymbol{A}_1^{-1} \bar{\boldsymbol{A}}_1 \langle p_\alpha g_1(z_{d\alpha})\rangle \bar{\boldsymbol{B}}_1^T \boldsymbol{b} - \boldsymbol{B}_1 \boldsymbol{A}_1^{-1} \boldsymbol{N} \langle p_\alpha g_2(z_{d\alpha})\rangle \boldsymbol{B}_1^T \boldsymbol{b} \right.$$
$$\left. - \boldsymbol{B}_1 \boldsymbol{A}_1^{-1} \bar{\boldsymbol{N}} \langle p_\alpha g_3(z_{d\alpha})\rangle \bar{\boldsymbol{B}}_1^T \boldsymbol{b}\right] - \operatorname{Re}\left[\boldsymbol{B}_1 \langle p_\alpha\rangle \boldsymbol{A}_1^{-1} \boldsymbol{\Omega} g_4(z_d)\right],$$

where

$$g_1(z_{d\alpha}) = \frac{1}{z_{d\alpha} - \bar{z}_{d\alpha}}, \qquad\qquad g_2(z_{d\alpha}) = \frac{z_{d\alpha} - \sqrt{z_{d\alpha}^2 - a^2}}{z_{d\alpha}^2 - a^2},$$

$$g_3(z_{d\alpha}) = \frac{z_{d\alpha} - \bar{z}_{d\alpha} + \sqrt{z_{d\alpha}^2 - a^2} + \sqrt{\bar{z}_{d\alpha}^2 - a^2}}{(z_{d\alpha} - \bar{z}_{d\alpha})\sqrt{z_{d\alpha}^2 - a^2}}, \qquad g_4(z_d) = \frac{z_d}{\sqrt{z_d^2 - a^2}},$$

and the nonzero component ω of $\boldsymbol{\Omega}$ is obtained from Equation (93) by deleting the first term due to the remote loads.

For the case in which Y is complex, from Equations (2), (3), and (113), one has

$$\boldsymbol{\Phi}_{,1}^d = \frac{1}{\pi} \operatorname{Im}\left[\boldsymbol{B}_1 \boldsymbol{A}_1^{-1} (\bar{\boldsymbol{A}}_1 - 2\bar{\boldsymbol{N}}) \langle g_1(z_{d\alpha})\rangle \bar{\boldsymbol{B}}_1^T \boldsymbol{b}\right] + 2 \operatorname{Re}\left[\boldsymbol{B}_1 \boldsymbol{A}_1^{-1} \sum_{\alpha=1}^4 \frac{\lambda_\alpha^d(z_d)\boldsymbol{\Lambda}_\alpha}{(1 + e^{2\pi\varepsilon_\alpha})v_\alpha}\right],$$

$$\boldsymbol{\Phi}_{,2}^d = \frac{1}{\pi} \operatorname{Im}\left[\boldsymbol{B}_1 \boldsymbol{A}_1^{-1} (\bar{\boldsymbol{A}}_1 - 2\bar{\boldsymbol{N}}) \langle p_\alpha g_1(z_{d\alpha})\rangle \bar{\boldsymbol{B}}_1^T \boldsymbol{b}\right] + 2 \operatorname{Re}\left[\boldsymbol{B}_1 \langle p_\alpha\rangle \boldsymbol{A}_1^{-1} \sum_{\alpha=1}^4 \frac{\lambda_\alpha^d(z_d)\boldsymbol{\Lambda}_\alpha}{(1 + e^{2\pi\varepsilon_\alpha})v_\alpha}\right],$$

where the nonzero component ω of $\boldsymbol{\Omega}$ is obtained from Equation (111) by deleting the last term due to the remote loads and $\lambda_\alpha^d(z_d)$ can be found from (110) by letting $z \to z_d$.

7.2. *A single rigid dielectric line.* For the case in which Y is real, from Equations (2), (3), and (101), one has

$$\Phi_{,1}^d = \frac{1}{\pi} \operatorname{Im}\left[B_1 A_1^{-1}(\bar{A}_1 - 2\bar{N})\langle g_1(z_{d\alpha})\rangle \bar{B}_1^T b - B_1 A_1^{-1}(\hat{I} - E)\hat{N}\langle g_2(z_{d\alpha})\rangle B_1^T b \right.$$

$$\left. + B_1 A_1^{-1}(\hat{I} - E)\bar{\hat{N}}\langle g_5(z_{d\alpha})\rangle \bar{B}_1^T b \right] - \operatorname{Re}\left[B_1 A_1^{-1}(\hat{I} - E)\hat{\Omega} g_4(z_d)\right],$$

$$\Phi_{,2}^d = \frac{1}{\pi} \operatorname{Im}\left[B A_1^{-1}(\bar{A}_1 - 2\bar{N})\langle p_\alpha g_1(z_{d\alpha})\rangle \bar{B}_1^T b - B A_1^{-1}(\hat{I} - E)\hat{N}\langle p_\alpha g_2(z_{d\alpha})\rangle B_1^T b \right.$$

$$\left. + B A_1^{-1}(\hat{I} - E)\bar{\hat{N}}\langle p_\alpha g_5(z_{d\alpha})\rangle \bar{B}_1^T b \right] - \operatorname{Re}\left[B\langle p_\alpha\rangle A_1^{-1}(\hat{I} - E)\hat{\Omega} g_4(z_d)\right],$$

where

$$g_5(z_{d\alpha}) = \frac{z_{d\alpha} + \bar{z}_{d\alpha} - \sqrt{z_{d\alpha}^2 - a^2} - \sqrt{\bar{z}_{d\alpha}^2 - a^2}}{\left(\sqrt{z_{d\alpha}^2 - a^2} + \sqrt{\bar{z}_{d\alpha}^2 - a^2}\right)\sqrt{z_{d\alpha}^2 - a^2}},$$

and the nonzero component ω of $\hat{\Omega}$ is obtained from Equation (100) by deleting the first term due to the remote loads.

For the case in which Y is complex, we have from Equations (2), (3), and (119)

$$\Phi_{,1}^d = \frac{1}{\pi} \operatorname{Im}\left[B_1 A_1^{-1}(\bar{A}_1 - 2\bar{N})\langle g_1(z_{d\alpha})\rangle \bar{B}_1^T b \right] + 2\operatorname{Re}\left[B_1 A_1^{-1}(\hat{I} - E)\sum_{\alpha=1}^3 \frac{\lambda_\alpha^d(z_d)\Lambda_\alpha}{(1 + e^{2\pi\varepsilon_\alpha})v_\alpha}\right],$$

$$\Phi_{,2}^d = \frac{1}{\pi} \operatorname{Im}\left[B_1 A_1^{-1}(\bar{A}_1 - 2\bar{N})\langle p_\alpha g_1(z_{d\alpha})\rangle \bar{B}_1^T b \right] + 2\operatorname{Re}\left[B_1\langle p_\alpha\rangle A_1^{-1}(\hat{I} - E)\sum_{\alpha=1}^3 \frac{\lambda_\alpha^d(z_d)\Lambda_\alpha}{(1 + e^{2\pi\varepsilon_\alpha})v_\alpha}\right],$$

where the nonzero component ω of $\hat{\Omega}$ is obtained from Equation (117) by deleting the last term due to the remote loads, and $\lambda_\alpha^d(z_d)$ can be found from (116) by let $z \to z_d$.

8. Numerical examples and discussions

In this section, numerical examples are performed to show a) the singularity types of the near-tip stress and electric displacement field, as well as b) to examine the effects of such parameters as the position of the mixed dislocation, and the Burgers vector components b_1, b_2, b_φ, on the image force. As an example, BaTiO$_3$ is considered for s_1 and PZT-6B for s_2, with material properties listed in Table 1 [Ou and Wu 2003]. Poling directions of the two materials are assumed to be along the x_2 axis. Based on the material constants given, we obtain

$$\varepsilon = 0, \qquad \kappa = 0.03528, \tag{122}$$

$$\Lambda_A = \begin{bmatrix} 0 & 0 & 3.506 \times 10^{-10} & -3.506 \times 10^{-10} \\ 0 & -1.6807 \times 10^{-9} & -2.245 \times 10^{-10} & -2.245 \times 10^{-10} \\ 1 & 0 & 0 & 0 \\ 0 & 0.9999 & 0.9999 & 0.9999 \end{bmatrix}$$

		PZT-6B	BaTiO$_3$
c_{11}	GPa	168	150
c_{12}	GPa	60	66
c_{13}	GPa	60	66
c_{33}	GPa	163	146
c_{44}	GPa	27.1	44
e_{31}	C/m^2	-0.90	-4.35
e_{33}	C/m^2	7.10	17.5
e_{15}	C/m^2	4.60	11.4
ε_{11}	10^{-10}C/Vm	36.0	98.7
ε_{13}	10^{-10}C/Vm	34.0	112

Table 1. Material Properties for BaTiO$_3$ and PZT-6B. The poling direction is along the x_3 axis.

for the conducting case, and

$$\varepsilon = 0.02439, \tag{123}$$

$$\mathbf{\Lambda}_A = \begin{bmatrix} 0.7315 & 0.7315 & 0 \\ 0.6818i & -0.6818i & 0 \\ 0 & 0 & 1 \end{bmatrix}$$

for the dielectric case.

For BaTiO$_3$/PZT-6B bimaterial, it is found from Equations (58), (63), and (122) that the stress and electric displacement fields at the rigid conducting line tips present square root and nonsquare root singularities. It is also observed from Equations (76) and (123) that the stress and electric displacement fields at the rigid dielectric line tips have square root and oscillatory singularities, for BaTiO$_3$/PZT-6B and other piezoelectric materials.

Here, the tangential and radial components of the image force are analyzed, given by

$$F_t = -F_x \sin[\theta_d] + F_y \cos[\theta_d], \qquad F_r = F_x \cos[\theta_d] + F_y \sin[\theta_d].$$

The normalizing factors are taken as

$$F_0(b_i) = \frac{1}{4\pi a} \boldsymbol{b}^T \boldsymbol{L}_1 \boldsymbol{b}, \qquad i = 1, 2, 4,$$

for nonzero b_i. Thus the normalized tangential and radial components of the image force are given by

$$F_t^*(b_i) = F_t(b_i)/F_0(b_i), \qquad F_r^*(b_i) = F_r(b_i)/F_0(b_i), \qquad i = 1, 2, 4,$$

where a positive term contributes to the repulsive force and a negative term to the attractive force.
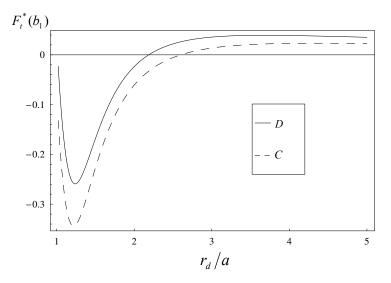
Figure 2. Normalized tangential force $F_t^*(b_1)$ versus r_d/a for $\theta_d = \pi/8$.

Normalized forces $F_t^*(b_1)$, $F_r^*(b_1)$, $F_t^*(b_2)$, $F_r^*(b_2)$, $F_t^*(b_\varphi)$ and $F_r^*(b_\varphi)$ versus r_d/a are depicted in Figures 2–7, respectively, for $\theta_d = \pi/8$. Normalized forces $F_t^*(b_1)$, $F_r^*(b_1)$, $F_t^*(b_2)$, $F_r^*(b_2)$, $F_t^*(b_\varphi)$ and $F_r^*(b_\varphi)$ versus θ_d, for $r_d = 1.5a$, are plotted in Figures 8–13, respectively. The symbols C and D in the figures stand for the conducting and dielectric cases, respectively.

In the tangential direction, it is seen from Figure 2 that the interface and the rigid dielectric lines attract the dislocation with b_1 at a point (r_d, θ_d) when $r_d/a < \hat{r}_1^*$, and repel the dislocation with b_1 at a point (r_d, θ_d) when $r_d/a > \hat{r}_1^*$. The same phenomenon can be observed if $\hat{r}_1^*$ is replaced by $\hat{r}_2^*$ $(\hat{r}_2^* > \hat{r}_1^*)$ for the conducting case. It is also found that the attractive force is stronger and the repulsive force is weaker

Figure 3. Normalized radial force $F_r^*(b_1)$ versus r_d/a for $\theta_d = \pi/8$.
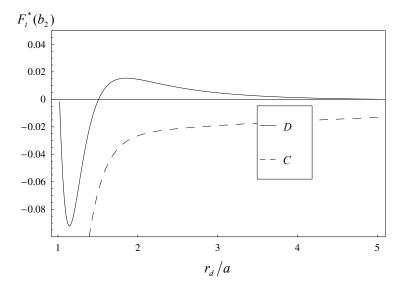
Figure 4. Normalized tangential force $F_t^*(b_2)$ versus r_d/a for $\theta_d = \pi/8$.

for the conducting case than for the dielectric case. The opposite phenomenon is observed from Figure 3 in the radial direction, where $\hat{r}_1^*$ and $\hat{r}_2^*$ are replaced by $\hat{r}_3^*$ and $\hat{r}_4^*$ ($\hat{r}_4^* > \hat{r}_3^*$), respectively.

As shown in Figure 4, in the tangential direction, the interface and the rigid conducting line always attract the dislocation with b_2. However, the interface and the rigid dielectric line repel the dislocation with b_2 at a point (r_d, θ_d) when $r_d/a < \hat{r}_5^*$ or $r_d/a > \hat{r}_6^*$ ($\hat{r}_6^* > \hat{r}_5^*$), and attract the dislocation with b_2 at a point (r_d, θ_d) when $\hat{r}_5^* < r_d/a < \hat{r}_6^*$, in the tangential direction. Moreover from Figure 4, it should be noted that the attractive force on a dislocation with b_2 is stronger for the conducting case than for the dielectric case along the tangential direction. We can observe from Figure 5 that the interface and the
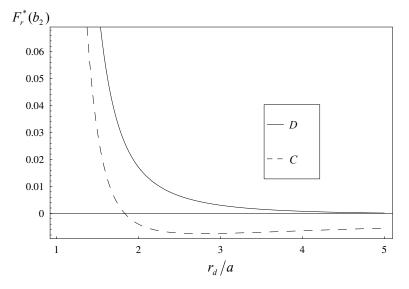

Figure 5. Normalized radial force $F_r^*(b_2)$ versus r_d/a for $\theta_d = \pi/8$.
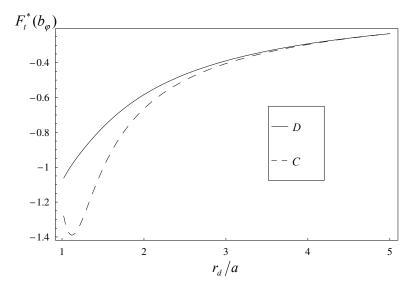
Figure 6. Normalized tangential force $F_t^*(b_\varphi)$ versus r_d/a for $\theta_d = \pi/8$.

rigid dielectric line always repel the dislocation with b_2, in the radial direction. However, the interface and the rigid conducting line repel the dislocation with b_2 at a point (r_d, θ_d) when $r_d/a < \hat{r}_7^*$, and attract the dislocation with b_2 at a point (r_d, θ_d) when $r_d/a > \hat{r}_7^*$, in the radial direction. Also it can be observed that the rigid dielectric line repels the dislocation with b_2 more strongly than the rigid conducting line does.

In the tangential direction, it is clear from Figure 6 that the rigid conducting line induces a stronger attractive force on the dislocation with b_φ than does the rigid dielectric line. In the radial direction, it is observed from Figure 7 that the interface and the rigid dielectric line always attract the dislocation with
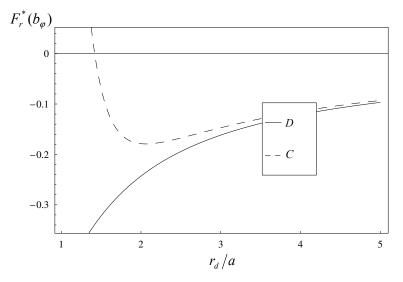

Figure 7. Normalized radial force $F_r^*(b_\varphi)$ versus r_d/a for $\theta_d = \pi/8$.
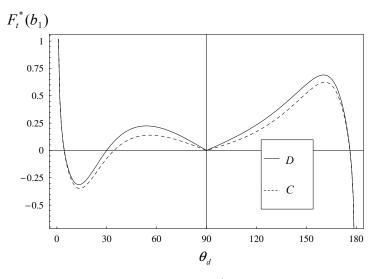
$F_t^*(b_1)$

Figure 8. Normalized tangential force $F_t^*(b_1)$ versus θ_d for $r_d = 1.5a$.

b_φ. However, the interface and the rigid conducting line repel the dislocation with b_φ at a point (r_d, θ_d) when $r_d/a < \hat{r}_8^*$ and attract the dislocation with b_φ at a point (r_d, θ_d) when $r_d/a > \hat{r}_8^*$. Further, we observe from Figure 7 that the rigid dielectric line always attracts the dislocation with b_φ more strongly than does the rigid conducting line in the radial direction.

It is seen from Figure 8 that the value of the tangential force on a dislocation with b_1 away from the interface is always larger for the dielectric case than for the conducting case. This means that the effects on the forces due to the rigid dielectric line (the repulsive force is stronger and the attractive force is weaker) are stronger than the effects on the forces due to the rigid conducting line. From Figure 9, it can be observed that the value of the radial force on a dislocation with b_1 at a point (r_d, θ_d), in which
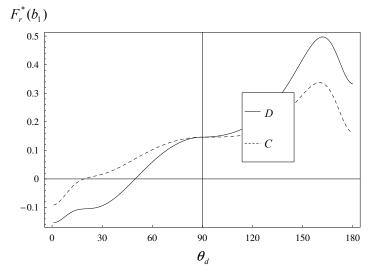
$F_r^*(b_1)$

Figure 9. Normalized radial force $F_r^*(b_1)$ versus θ_d for $r_d = 1.5a$.
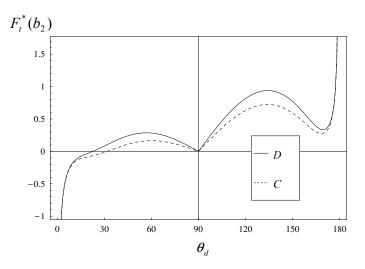
$F_t^*(b_2)$

Figure 10. Normalized tangential force $F_t^*(b_2)$ versus θ_d for $r_d = 1.5a$.

$\theta_d < 90°$, is always larger for the conducting case than for the dielectric case. However, the opposite phenomenon is observed when $90° < \theta_d < 180°$.

The force on a dislocation with b_2, which repels the dislocation away from the interface (as is seen from Figure 10), is stronger due to a rigid dielectric line than the force due to a rigid conducting line in the tangential direction. The same phenomenon is observed from Figure 11 for the case $\theta_d < 90°$ in the radial direction. It is also observed that the value of the radial force increases with increasing θ_d ($\theta_d < 90°$ or $\theta_d > 90°$).

It can be observed from Figure 12 that the attractive force on a dislocation with b_φ, at a point (r_d, θ_d) when $\theta_d < 90°$, is always stronger for the rigid conducting line case than for the rigid dielectric line, in the tangential direction. Figure 12 also shows that the rigid dielectric line repels a dislocation with b_φ
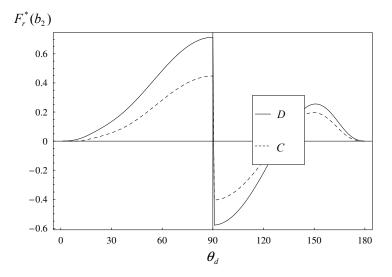
$F_r^*(b_2)$

Figure 11. Normalized radial force $F_r^*(b_2)$ versus θ_d for $r_d = 1.5a$.
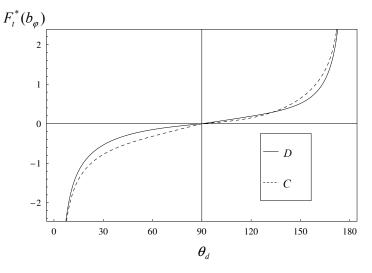
Figure 12. Normalized tangential force $F_t^*(b_\varphi)$ versus θ_d for $r_d = 1.5a$.

at a point (r_d, θ_d) more strongly than does the rigid conducting line, when $90° < \theta_d < \theta_d^*$. The opposite phenomenon can be observed at a point (r_d, θ_d), when $\theta_d^* < \theta_d < 180°$. It is worth noting that the value of the tangential force increases with an increase in θ_d. Figure 13 clearly shows that the interface and the rigid dielectric line always attract a dislocation with b_φ in the radial direction, and the value of the radial force is always larger for the conducting case than for the dielectric case.

It is worth noting from Figures 2–7 that the image forces on the dislocation, which move it away from the interface along the radial direction, approach the same value gradually, and become zero ultimately for the two cases. This is due to the fact that the remarkable distance between the dislocation and the interface weakens the interaction between the dislocation and the rigid lines. It can be observed from
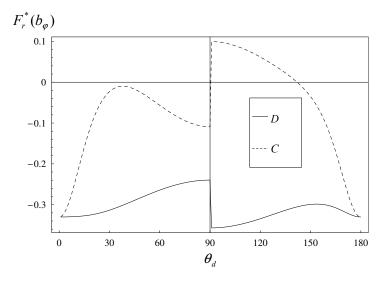

Figure 13. Normalized radial force $F_r^*(b_\varphi)$ versus θ_d for $r_d = 1.5a$.

Figures 8, 10, and 12 that the tangential forces on the dislocation near the interface approach the same value for the two cases, which indicates that the interaction between the dislocation and the interface is dominant. From Figures 11 and 13, a large change of the radial force acting on a dislocation near the point $z^*(1.5a, \ 90°)$ is observed due to the electroelastic interaction. The dislocation with b_1 at $z^*(1.5a, \ 90°)$ for the dielectric and conducting cases in equilibrium is also observed in the examples.

9. Conclusion

The Stroh formalism was employed to analyze the interaction between a piezoelectric dislocation and the collinear rigid lines, which are either conducting or dielectric, at the interface of two piezoelectric media. The general solutions for the field variables were obtained. A square root singularity was identified for the stress and electric displacement fields at the tips of interfacial rigid conducting/dielectric lines when the two piezoelectric media have sufficient symmetry so that the matrix Y is real. It was further found that the stress and electric displacement fields at the tips of interfacial rigid conducting lines present either a combination of square root and oscillatory singularities or a combination of square root and nonsquare root singularities in transversely isotropic piezoelectric media where the matrix Y is complex, or a combination of oscillatory and nonsquare root singularities in piezoelectric media whose material properties do not match suitably, so that the real numbers $\varepsilon \neq 0$ and $\kappa \neq 0$. The fields at the tips of rigid dielectric lines have square root and oscillatory singularities at the interface of a piezoelectric bimaterial system where the matrix Y is complex. The strain and electric field intensity factors were introduced to characterize the near-tip field singularity. The expressions of the rigid line extension forces, based on the energy release rate and the mechanical energy release rate, were derived. The exact field solutions for the case of a single interfacial rigid line were presented. The effects of the Burgers vector and the dislocation position on the image force were analyzed in detail.

References

[Asundi and Deng 1995] A. Asundi and W. Deng, "Rigid inclusions on the interface between dissimilar anisotropic media", *J. Mech. Phys. Solids* **43** (1995), 1045–1058.

[Ballarini 1990] R. Ballarini, "A rigid line inclusion at a bimaterial interface", *Eng. Fract. Mech.* **37** (1990), 1–5.

[Beom 2003] H. G. Beom, "Permeable cracks between two dissimilar piezoelectric materials", *Int. J. Solids Struct.* **40** (2003), 6669–6679.

[Beom and Atluri 2002] H. G. Beom and S. N. Atluri, "Conducting cracks in dissimilar piezoelectric media", *Int. J. Fract.* **118** (2002), 285–301.

[Chen et al. 2005a] B. J. Chen, K. M. Liew, and Z. M. Xiao, "A dislocation interacts with a finite crack in piezoelectric media", *Int. J. Eng. Sci.* **43** (2005a), 1206–1222.

[Chen et al. 2005b] B. J. Chen, K. M. Liew, and Z. M. Xiao, "Unified electrical boundary conditions for a crack interacting with a dislocation in piezoelectric media", *Int. J. Solids Struct.* **42** (2005b), 5118–5128.

[Chen et al. 2007] B. J. Chen, D. W. Shu, and Z. M. Xiao, "Dislocation interacting with collinear rigid lines in piezoelectric media", *Journal of Mechanics of Materials and Structures* **2**:1 (2007), 23–42.

[Deng and Meguid 1998] W. Deng and S. A. Meguid, "Analysis of conducting rigid inclusion at the interface of two dissimilar piezoelectric materials", *J. Appl. Mech. (Trans. ASME)* **65** (1998), 76–84.

[Fang et al. 2005] Q. H. Fang, Y. W. Liu, and C. P. Jiang, "Electroelastic interaction between a piezoelectric screw dislocation and an elliptical inclusion with interfacial cracks", *Phys. Status Solidi (b)* **242** (2005), 2775–2794.

[Gao et al. 2005] C.-F. Gao, P. Tong, and T.-Y. Zhang, "Interaction of a dipole with an interfacial crack in piezoelectric media", *Compos. Sci. Technol.* **65** (2005), 1354–1362.

[Hausler et al. 2004] C. Hausler, C.-F. Gao, and H. Balke, "Collinear and periodic electrode-ceramic interfacial cracks in piezoelectric bimaterials", *J. Appl. Mech. (Trans. ASME)* **71** (2004), 486–492.

[Jiang 1991] C.-P. Jiang, "The plane problem of collinear rigid lines under arbitrary loads", *Eng. Fract. Mech.* **39** (1991), 299–308.

[Jiang and Liu 1992] C. P. Jiang and C. T. Liu, "Stress distribution around a rigid line in dissimilar media", *Eng. Fract. Mech.* **42** (1992), 27–32.

[Li and Ting 1989] Q. Li and T. C. T. Ting, "Line inclusions in anisotropic elastic solids", *J. Appl. Mech. (Trans. ASME)* **56** (1989), 556–563.

[Liu et al. 2004] Y. W. Liu, Q. H. Fang, and C. P. Jiang, "A piezoelectric screw dislocation interacting with an interphase layer between a circular inclusion and the matrix", *Int. J. Solids Struct.* **41** (2004), 3255–3274.

[Meguid and Deng 1998] S. A. Meguid and W. Deng, "Electro-elastic interaction between a screw dislocation and an elliptical inhomogeneity in piezoelectric materials", *Int. J. Solids Struct.* **35** (1998), 1467–1482.

[Muskhelishvili 1975] N. I. Muskhelishvili, *Some basic problems of the mathematical theory of elasticity: fundamental equations plane theory of elasticity torsion and bending*, Fourth Edition ed., P. Noordhoff, Leyden, Holland, 1975.

[Ou and Wu 2003] Z. C. Ou and X. Wu, "On the crack-tip stress singularity of interfacial cracks in transversely isotropic piezoelectric bimaterials", *Int. J. Solids Struct.* **40** (2003), 7499–7511.

[Pak 1990a] Y. E. Pak, "Crack extension force in a piezoelectric material", *J. Appl. Mech. (Trans. ASME)* **57** (1990a), 647–653.

[Pak 1990b] Y. E. Pak, "Force on a piezoelectric screw dislocation", *J. Appl. Mech. (Trans. ASME)* **57** (1990b), 863–869.

[Ru 2000] C. Ru, "Electrode-ceramic interfacial cracks in piezoelectric multilayer materials", *J. Appl. Mech. (Trans. ASME)* **67** (2000), 255–261.

[Sosa and Pak 1990] H. A. Sosa and Y. E. Pak, "Three-dimensional eigenfunction analysis of a crack in a piezoelectric material", *Int. J. Solids Struct.* **26** (1990), 1–15.

[Suo 1990] Z. Suo, "Singularities, interfaces and cracks in dissimilar anisotropic media", pp. 331–358 in *Proceedings of the Royal Society of London*, edited by 427, Series A, Mathematical and Physical Sciences, 1990.

[Suo et al. 1992] Z. Suo, C.-M. Kuo, D. M. Barnett, and J. R. Willis, "Fracture mechanics for piezoelectric ceramics", *J. Mech. Phys. Solids* **40** (1992), 739–765.

[Wang and Shen 2002] X. Wang and Y.-p. Shen, "Exact solution for mixed boundary value problems at anisotropic piezoelectric bimaterial interface and unification of various interface defects", *Int. J. Solids Struct.* **39** (2002), 1591–1619.

[Wu 1990] K.-C. Wu, "Line inclusions at anisotropic bimaterial interface", *Mech. Mater.* **10** (1990), 173–182.

[Xiao and Zhao 2004] Z. M. Xiao and J. F. Zhao, "Electro-elastic stress analysis for a Zener-Stroh crack at the metal/piezoelectric bi-material interface", *Int. J. Solids Struct.* **41** (2004), 2501–2519.

[Xiao et al. 2004] Z. M. Xiao, J. Yan, and B. J. Chen, "Electro-elastic stress analysis for a screw dislocation interacting with a coated inclusion in piezoelectric solid", *Acta Mech.* **172** (2004), 237–249.

[Xiao et al. 2007] Z. M. Xiao, H. X. Zhang, and B. J. Chen, "A piezoelectric screw dislocation interacts with interfacial collinear rigid lines in piezoelectric bimaterials", *Int. J. Solids Struct.* **44** (2007), 255–271.

ZHONGMIN XIAO: mzxiao@ntu.edu.sg
School of Mechanical and Aerospace Engineering, Nanyang Technological University, Nanyang Avenue, Singapore 639798

HONGXIA ZHANG: mhzhang@ntu.edu.sg
School of Mechanical and Aerospace Engineering, Nanyang Technological University, Nanyang Avenue, Singapore 639798

BINGJIN CHEN: mbchen@ntu.edu.sg
School of Mechanical and Aerospace Engineering, Nanyang Technological University, Nanyang Avenue, Singapore 639798